1966

Sensible heat sources using fission products

Donald Porter Naismith
Iowa State University

SENSIBLE HEAT SOURCES USING FISSION PRODUCTS

by

Donald Porter Naismith

A Dissertation Submitted to the
Graduate Faculty in Partial Fulfillment of
The Requirements for the Degree of
DOCTOR OF PHILOSOPHY

Major Subject: Nuclear Engineering

Approved:

Signature was redacted for privacy.
In Charge of Major Work

Signature was redacted for privacy.
Head of Major Department

Signature was redacted for privacy.
Dean of Graduate College

Iowa State University
Of Science and Technology
Ames, Iowa

1966

TABLE OF CONTENTS

INTRODUCTION

The emanations from radioactive atoms have long been recognized as a source of energy (1), but until recent times there has been little serious effort put forth to use radiation this way. The beginning of the Systems for Nuclear Auxiliary Power (SNAP) program in 1955 and its subsequent efforts no doubt have had the greatest single effect toward increasing activity in the use of isotopes for thermal power (2). A search of the literature and the number of related references gives a good indication of the increasing activity. Prior to 1960 there are very few articles of consequence with the number increasing at a rapidly increasing rate since then. Based on the projected rate of accumulation of waste fission products, the thermal power available from radioisotopes has increased from about 50 kw/yr in 1963 to 227 kw estimated for 1966 to 1200 kw projected for 1970. The increased demand for isotopes is sufficiently great that the AEC production activity has recently taken steps to meet the challenge (3).

In general there have been two major categories of radioisotopes considered for thermal applications: the beta-emitting fission products which have been separated and the most energetic of the alpha particle emitters. Gross or mixed fission products have been dismissed because of low power densities (watts/cc) and shielding difficulties. Until the past year or two only a few beta emitters and a few alpha emitters have appeared economical (4). However, several isotopes such as Tl - 204 and Tm - 170 have advantages great enough to

Table 1. Isotopic power sources

Beta emitters	Alpha emitters
Sr - 90	Pu - 238
Cs - 137	Cm - 244
Ce - 144	Cm - 242
Pm - 147	Po - 210

warrant further study of the separation processes and the Battelle - Northwest Laboratories are presently spending considerable effort on improved processing. They feel there is real promise for isotopic heat sources (4, 5, 6, 7, 8, 9).

Work on converting liquid radioactive wastes to solids by calcination has been increased. It is reasonable to expect that such methods will be common in the near future and that calcined mixed fission products with densities of 1.0 - 3.0 g/cc and with power densities in the vicinity of 0.20 watts/cc produced from 10,000 Mwd/tonne reactor fuels will be available (10, 11). This thesis is concerned with the preliminary design of a heater to make use of this form of fission products.

Literature Review

One of the more closely related references is the feasibility study of a radioisotopic power source for remote area heating which

was done by Chance - Vought Corporation in 1962 (12). They investigated the technical and economic feasibility of units of 50,000 and 300,000 Btu/hr with a life of 10 years. Consideration was given to energy sources, thermodynamic cycles, design concepts, safety, and economics. Sr - 90 was chosen as the fuel for their study because of its long life, availability and small shielding requirements. The 3.9 megacuries (50,000 Btu/hr model) of Sr - 90 titanate was to be vibration packed into a Hastelloy C cylinder to form the fuel element. The fuel element was surrounded by a close fitting depleted uranium shield which was clad on the outside with an extended aluminum, finned surface. Simplicity of manufacture was of considerable concern throughout the design. Two operation cycles were considered. One used air and the other boiling water; in either case they were designed to be cooled by natural circulation should a power failure occur. The following summary of the specifications will assist in forming a mental picture of the proposed device.

Table 2. Summary of design specifications for strontium titinate heater of reference (12)

Output	Life	Fuel			Shield thickness uranium	Weight of heater
Btu/hr	yr	$Sr^{90}TiNO_3$ megacuries	Volume ft^3	Weight lb	in.	lb
50,000	10	3.866	0.683	213	4.67	4,350
300,000	10	23.2	4.10	1278	4.72	10,900

The safety analysis for this design consisted of radiobiological considerations and the hazard aspects of fabrication, transportation, and operation. The shield design was based on Interstate Commerce Commission regulations, parts 71 through 78 of Title 49, Code of Federal Regulations, which specifies an allowable gamma dose of 200 mr/hr at any accessible surface and 10 mr/hr at one meter. This shield was designed to serve as the shipping container for the unit. Once the fuel was loaded into the unit it was required that it have auxiliary power for operation of the cooling fans or pumps. Emergency operation was defined as the condition when auxiliary power was not available. It was calculated that the temperature at the center of the fuel, at the outside of the fuel, and at the outside of the shield would be 1972°F, 930°F and 388°F respectively for indefinite emergency operation with the air cycle. Cooling in this case was provided by natural convection chimney effect. The maximum credible incident was proposed as a blocked coolant flow or exposure to a fire, either of which might cause a melt down and result in dose rates on the order of 200,000 R/hr. Based on their assumptions they calculated the loss of coolant would not cause a melt down of the shield for 24 hr after the loss occurred. Based on the standard fire criterion of a temperature of 1750°F for one hour and with the fan inoperable the shield would not melt and would revert to emergency operation if there was no blockage of the coolant passage. As a most serious condition they proposed an incident where 10,000 gallons of gasoline, as in a tank car, might surround the unit

and burn. With aluminum fins, the shield would be lost, however, they postulated that stainless steel fins could make the unit nearly fireproof.

The economic analysis was based on breaking even with system costs for equivalent output, oil-fired heating systems in a remote arctic area. By using two 50,000 Btu/hr systems and proper source combinations for a total life of 55 years, the allowable cost of the Sr - 90 was reduced to $65.00 per kilocurie. At the time of the study, Sr - 90 was available at $5.00 per curie and presently it is available for $0.20 per curie in large quantities (13). It is obvious that radioisotope costs have been substantially reduced and it is reasonable to expect further reduction.

The important conclusions of this feasibility study are

1. The nuclide heat concept is technically feasible.
2. The nuclide heat concept will be economical in remote areas when radioisotopes are available at approximately $0.07 per curie.
3. The system can be built and operated safely under existing regulations for handling radioisotopes.
4. The air cycle concept is the most promising when design, operation, safety, and reliability are considered.

In addition, the waste management aspect of isotopic heaters can not be ignored and may make these heaters economically desirable, especially to governmental departments.

Chance - Vought Corporation has also done work on using isotopes as a source of heat for distilling sea water (14). This study consisted of three main parts.

1. An economic feasibility study in which they conclude the most economical source appears to be calcined fission products which, for special conditions, is competitive with conventional fuels.

2. A conceptual design including compatability, thermodynamics, nuclear, and material aspects of a one million gallon per day plant.

3. The design of a laboratory test model using one megacurie of Ce - 144 and multistage flash evaporation to produce 250 gallons of water per day.

The primary differences in costs associated with a design using radioisotopes result from source preparation and handling, shipping casks, and transportation. Since there was relatively little experience in preparing and using megacurie quantities, extrapolations of the existing technology were used. The distance from the nearest fuel processing plant was a deciding factor and for a given set of conditions (400 days decay time, 2,000 day use cycle) a distance of about 600 miles became a break-even point with conventional steam plants. The cost of the fuel varied from $0.55 to $0.95 per million Btu depending on the distance. This compared favorably with gasoline, kerosine, and fuel oil and means that converted saline water in the continental U. S. would cost from $0.70 to $0.85 per 1,000 gallons. In comparison, the national average cost of water from public utilities (domestic and commercial) is $0.32 per 1,000 gallons..

The technical feasibility of using radioisotopes for desalting water was investigated by first determining what a large scale plant might look like and trying to predict what its operation would be. After this step, a laboratory test model to prove the principles was constructed. Thermodynamic and heat transfer studies were conducted on various fuel configurations. Some of the assumptions concerned with the source material are given in Table 3. Calculations and test

Table 3. Typical calcined fission product data for reference (14)

Item	Calcined gross fission products	Sintered calcined gross fission products
Reactor burnup MW days/tonne U	10,000	10,000
Waste recovery system	Purex	Purex
Volume recovered gallons/tonne U	10	10
Decay time days	300	300
Thermal conductivity Btu/hr/ft/^{o}F	0.4 - 0.6	0.4 - 0.6
Maximum design operating temperature ^{o}F	1,800	1,800
Density grams/cm^{3}	1.32	3.7
Specific activity curies/in.^{3}	312	875
Specific power watts/in.^{3}	2.15	6.0

data showed that the maximum diameter for a fuel element producing steam is between 7 and 8 inches while that for a gas (air) heater is

about 4 inches. Two heater systems were considered: a direct heater where salt water was in contact with the heater and an indirect system which used a closed primary heater loop. The indirect system had considerable advantage from a hazards point of view.

In summary, there is considerable work being done on small thermoelectric generators with high power density, small size, and small weight, viz., the SNAP devices. On the other hand, studies and models are under way for desalting water or providing remote areas with heat utilizing large isotopic heat sources. Both of these extremes are designed to use separated isotopes as the source of heat. In addition, another part of the technology shows considerable work is under way to reduce the waste fission product storage problem by use of calcined fission products.

A number of references have been reviewed which bear in some way on this particular design. These will be cited as they are used throughout the thesis.

Objective

The work presented and discussed in this thesis is concerned with the design of a safe, long-lived device which uses the decay energy of unseparated, calcined radioactive fission products for heating a fluid such as air. The heater is designed to produce 25,000 Btu/hr at temperatures up to 300°F for a design lifetime of 30 years.

Insofar as possible, technology which is in an advanced state of development or is well known is used. Certain of the data upon which

the design is based are quite likely to undergo revision and proof-of-principle experiments will undoubtedly be required before an experimental model is built. However, the primary factor in deciding the future for such a heater is the availability of heat source material.

The motivation for this work is two-fold. The first is the current search for dependable heat or power sources which are independent of logistics problems. The second factor is the currently increasing rate of waste product production from nuclear reactors for which storage is becoming a great problem. The radiations from these stored fission products represent a large quantity of wasted energy. The desire to adapt radioisotopes to another useful application and thereby promote the increase of peaceful uses of nuclear energy is also a motivation.

RADIOACTIVE WASTE SOURCES

The choice of using unseparated fission products as the radioactive source material for this heater design still leaves a number of decisions to be made. For instance, will the material be partially purified and as such be mixed fission products (MFP) or will it be used as gross fission products (GFP)? Once that decision is made the questions of physical form and period of decay before use are left. Even at this point the characteristics of the source material depend on such things as:

1. The specific power of the reactor the fuel elements came from.
2. The burnup and the time in the reactor.
3. The recovery process used.

A look at the work being done in radioactive waste processing shows that one of the more promising forms for the waste is calcined fission products. Some of the properties of these materials are known or are estimated by those working on the processing. Eaton (15, pp. 29 - 32) suggests that reactor fuels with burnups of 10,000 MW days/tonne at a power level of 33 MW/tonne will produce calcined oxides with activities of about 180,000 curies/pound or about 396,000 curies/kilogram. Table 4 shows a number of MFP calcined wastes and some of their physical properties.

Some properties can be controlled to a great extent, e.g., the value of the conductivity, k, can be changed appreciably by dilution

Table 4. Physical properties of mixed fission product calcined wastes

Process description	Calcination temp °C	Melting point °C	Density g/cm^3	Conductivity Btu/hr/ft/°F	Particle size mesh
ICPP fluidized bed aluminum type waste	400-500	1800	0.6-0.9	0.08-0.30	-28 + 35 37% -35 + 60 58 -60 + 100 5
HW fluidized bed Purex IWW	-------	800-1000	1.1-1.3	0.08-0.15	-20 + 100 80% -100 5
HW Spray calcination					
A. Purex	850	800-1000	0.8-0.9	0.05-0.13	Avg. 25 microns
B. TBP - 25	655	800	0.1	0.03	
C. (b) melted	---	800	2.2	---------	Dense glass
ORNL pot calcined Purex IWW	900	800-1000	1.0-3.0	0.2-2.4	Solid cake, variable consistency
HW pot calcined Purex IWW	850-900	800-1000	2.0-3.0	0.18-0.65	Solid cake, variable consistency

or by the addition of finely divided metal to the oxide mixture (14, 16). As one can see there is a great deal of variation in the properties and a choice of the best one at this time is probably not possible.

Reference to Figure 1 (11, p. 58) shows that after a decay period of about two years the ICPP wastes are almost entirely composed of the five isotopes listed in Table 5.

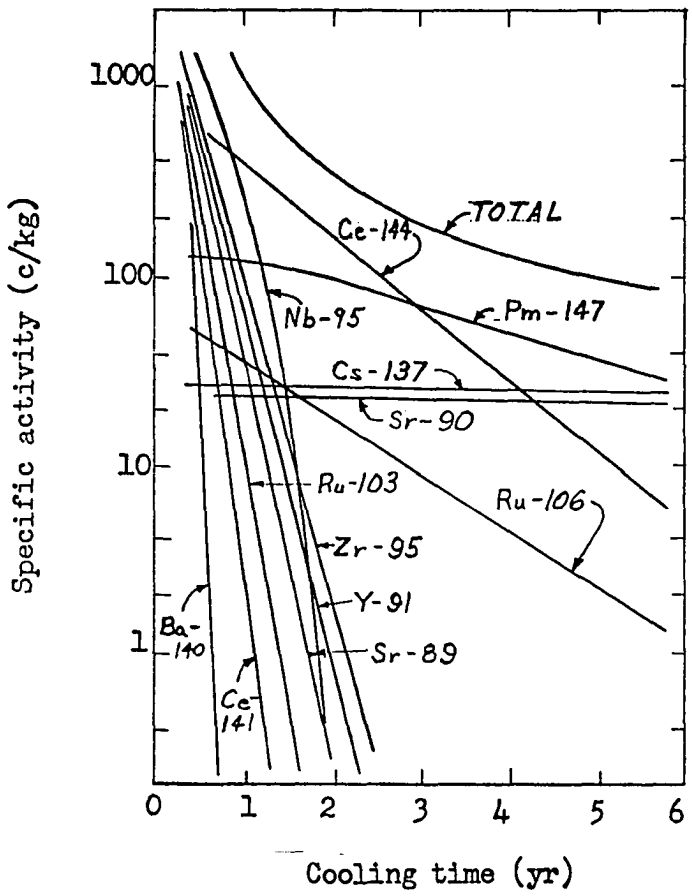

Figure 1. Specific activity of ICPP calcined wastes

Table 5. Calcined waste composition, two years decay

Isotope	Specific activity curies/kg	Composition %
Ce - 144	160.0	49.5
Pm - 147	96.0	29.7
Cs - 137	27.2	8.4
Sr - 90	23.1	7.1
Ru - 106	17.1	5.3
Total	323.4	

The lower band of Figure 2 (11, 15) shows the power densities for present technology with MTR type fuel elements and fluidized-bed calcination while the upper region is for projected "pot" calcination wastes.

It appears that HW pot calcinated Purex IWW wastes might be the most reasonable prospect for an energy source to be used in a fission product heater built in the immediate future (1968 - 1970).

There are other obvious advantages to the pot calcined wastes. Present calcination technology puts the material directly into cylindrical containers made of pipe. These containers are then sealed and stored (10, pp. 2 - 11). Other than the added expense of using a smaller container there seems to be little reason why such storage tubes could not be used directly in a device such as the fission-product heater. A second advantage is the stable form the product is in after

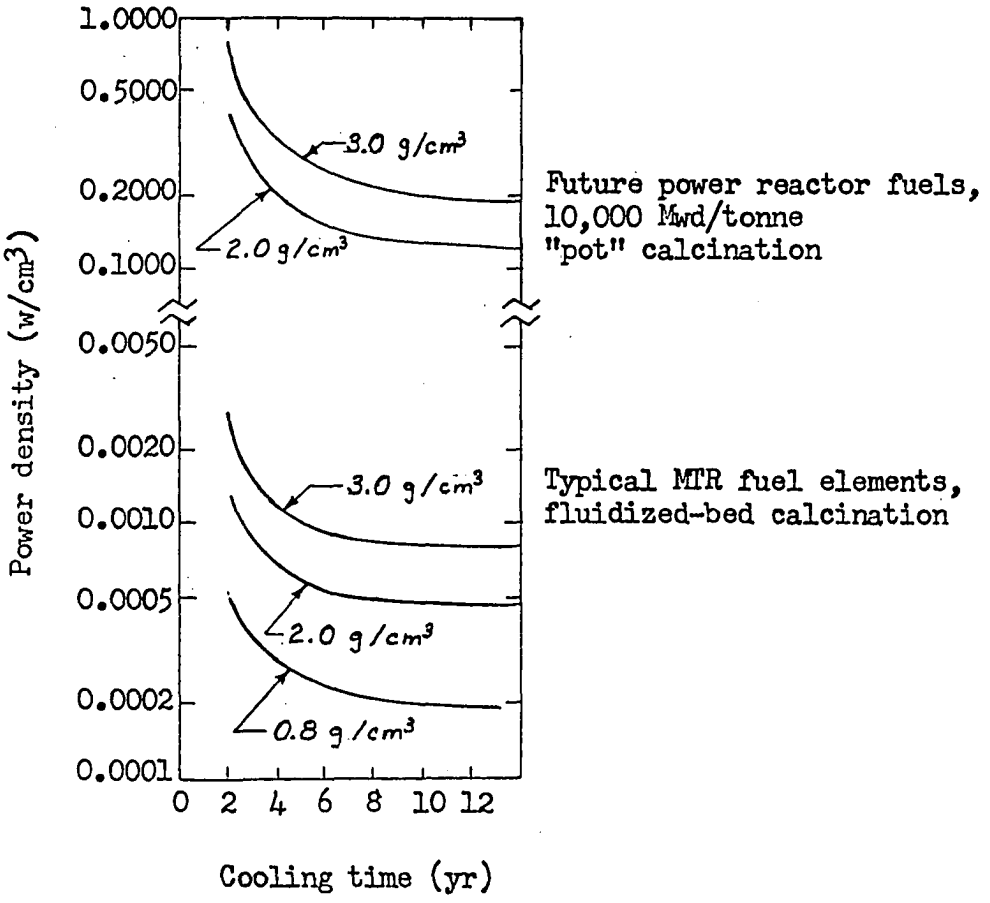

Figure 2. Power densities of mixed fission products (MFP) as a function of time.

calcination. However, the degree of radiation stability is unknown and some believe the residual nitrates may decompose to nitrogen and oxygen when operation takes the temperature near the calcination temperature. They also suggest the possibility of "getter" materials incorporated in the source to absorb the products of such decomposition (15, p. 27).

As a base for the design calculations the data in Table 6 are selected as representative of present or near-future technology.

Table 6. Source data for the fission product heater

Source material	HW Pot calcinated (Solid Cake) Purex IWW wastes from 10,000 MW days/tonne fuel
Density	2.4 grams/cubic centimeter
Specific weight	150 pounds/cubic foot
Specific activity	180,000 curies/pound

By extrapolation of Figure 2 to 30 years, the design lifetime, the power density is found to be about 0.15 watts/cm^3 whereas at the beginning (2 year decay time) the value is about 0.6 - 0.7 watts/cm^3. If the heater is to produce no less than 7500 watts (nominal 10 horsepower) throughout its life, the volume of the fuel can be estimated. With 100% energy removal, the volume of the fuel at the end of the cycle will be

$$\text{Volume} = \frac{7500}{0.15} = 50{,}000 \text{ cm}^3$$

$$= 1.767 \text{ ft}^3 \text{ or } 3{,}052 \text{ in.}^3$$

and its weight will be

$$\text{Weight} = (150)(1.767) = 265 \text{ lb}$$

At the beginning of the heaters life it will produce

$$\text{Power} = (50{,}000)\,(0.6) = 30{,}000 \text{ watts.}$$

The activity when the source is new will be

$$\text{Activity} = (1.8 \times 10^5)\,(265) = 47.7 \text{ megacuries (Mc)}$$

or about 15,620 curies/in.^{3}. This is in approximate agreement with the source proposed by Chance - Vought Corporation (12, pp. 69 - 70). They used 4 Mc of Sr - 90 $TiNO_3$ which has a power density of about 1.0 watts/cm^3.

If the source is assumed to be made up of the five sources listed in the proportions shown, an idea of how much of the energy is due to beta particle emission and how much is due to gamma ray emission can be obtained. References (17) and (18) provide data from which one can determine the power per kilocurie (Kc) due to beta particles and gamma rays for each isotope. Table 7 itemizes the data. The available gamma energy is about 9.4% of the total energy. If one includes Bremsstrahlung from beta particle interactions, the total photon energy is of the order of 10%. Reference (17) suggests that the Bremsstrahlung is small (about 0.16% of the beta energy for 1.5 mev beta particles) for such sources.

Probably a better approach to evaluating the photon energy of the source is to make use of fission product data available in reference (19). Use of these data requires a few more assumptions concerning power reactor operation since the waste depends on the fuel processed.

Table 7. Selected fission products and their properties

Isotope	Composition %	Specific activity Kc/in.^{3}	Beta particles		Gamma rays	
			watts/Kc	watts/in.^{3}	watts/Kc	watts/in.^{3}
Ce - 144 series	49.5	7.73	7.72	59.70	0.38	2.94
Pm - 147	29.7	4.64	0.38	1.76	-----	----
Cs - 137	8.4	1.31	1.60	2.10	3.20	4.20
Sr - 90	7.1	1.11	6.60	7.32	----	----
Ru - 106	5.3	0.83	8.65	7.16	1.20	0.99
			Total	78.04		8.13

For the purposes of this design the following values will be taken as representative of near-future power reactor operation:

1. Reactor operating flux, $\emptyset$ = 3 X 10^{13} neutrons/cm^2-sec
2. Reactor fuel enrichment = 2%
3. Fuel irradiation time = 3 X 10^7 sec (about 1 year)
4. Fuel burnup = 10,000 MW days/tonne.

Reference (17, pp. 2 - 11) indicates that 58 - 24 inch diameter tubes, 10 feet in length were filled with calcined Purex wastes per 1500 tonnes of uranium processed. This results in 3.05 gallons of calcined waste per tonne of uranium. The number of U - 235 atoms in the fuel, from which these wastes came, can be calculated.

Density = 2.4 g/cm^3

Source weight = 265 lb

Gallons of waste = 13.21 gal

Tonnes of uranium = 13.21/3.05 = 4.34 tonne

Weight of U - 235 = (4.34) (1000) (0.02) = 86.8 kg

Number of U - 235 atoms = $(86.8)\ (10^3)\ (0.6023 \times 10^{24})/235$

$= 22.15 \times 10^{25}$ atoms.

Table 8 gives the gamma ray data for four different initial decay periods. These data were determined using the preceding calculation and values given by reference (19). The values will be used throughout the calculations for shielding and gamma ray heating.

The total energy of the gamma radiation is about 6.9% of the total for 2-year decay while it decreases to 3.2% after 30 years of decay. Comparing with the previous estimate of 10%, it appears that the previously assumed composition is probably not quite correct. It is fortunate, however, that a relatively short decay time (2 years) significantly reduces the gamma problem and the source becomes 90% (or more) beta emitter.

Table 8. Fission product gamma ray data from (19)

Decay period sec	Gamma group	Energy of group mev	Effective energy mev	Gamma d/sec per U - 235 atom	Gamma energy rate mev/sec
3×10^{7}	I	0.00-0.25	0.125	1.1×10^{-10}	3.04×10^{15}
(1 yr)	II	0.25-1.00	0.67	2.8×10^{-10}	4.15×10^{16}
	III	1.0 -1.7	1.6	2.9×10^{-12}	1.03×10^{15}
	IV	1.7 -up	2.4	1.7×10^{-12}	9.03×10^{14}
6×10^{7}	I	0.00-0.25	0.125	3.4×10^{-11}	9.40×10^{14}
(2 yr)	II	0.25-1.0	0.67	7.5×10^{-11}	1.11×10^{16}
	III	1.0 -1.7	1.6	1.6×10^{-12}	5.65×10^{14}
	IV	1.7 -up	2.4	8.2×10^{-13}	4.35×10^{14}
1×10^{8}	I	0.00-0.25	0.125	1.9×10^{-11}	5.12×10^{14}
(3 yr)	II	0.25-1.0	0.67	2.7×10^{-11}	4.00×10^{15}
	III	1.0 -1.7	1.6	1.1×10^{-12}	3.90×10^{14}
	IV	1.7 -up	2.4	4.1×10^{-13}	2.18×10^{14}
1×10^{9}	I	0.00-0.25	0.125	4.6×10^{-14}	1.27×10^{12}
(30 yr)	II	0.25-1.0	0.67	9.8×10^{-12}	1.46×10^{15}
	III	1.0 -1.7	1.6	6.0×10^{-14}	2.12×10^{13}
	IV	1.7 -up	2.4	10^{-16} or less	5.30×10^{10}

HEATER DESIGN

There are many combinations of dimensions which would make a workable design. It seems likely that there is one, or at most a few, combinations which make a best design depending on how one defines best. A number of possibilities are to be investigated in this thesis; however, more information about the geometry and the materials to be used is required before the design calculations can proceed. Little conscious effort will be made to specify in detail the hardware required to build such a heater.

Geometry

The technology is being developed for calcinating fission products into cylindrical containers which are then sealed for waste disposal. Also, there are certain manufacturing advantages to cylindrical shapes. For these reasons the general shape of the heater was selected as a right circular cylinder with the source material contained within sealed tubes. These tubes will, in turn, be spaced within the heater. The source tubes are to be standard sized tubes (see Table 9) up to a maximum diameter of 4 inches as suggested in reference (14, p. 119). Each tube is to be provided with an annular coolant channel through which air will pass. The coolant channel will also provide the guide to maintain the source tubes in an upright position.

A convenient symmetric arrangement for the source tubes is a hexagonal array. The tubes will be supported from the bottom and will be free to expand axially and radially.

Table 9. Source tube specifications and data

Nominal OD in.	Inside radius in.	Wall thickness in.	Volume per ft $in.^3/ft$	Number of 3 ft lengths	Total rod length cm	Number of source rods
1 3/8	0.532	0.156	10.669	95.90	8770	96
1 1/2	0.594	0.156	13.301	76.90	7140	78
1 7/8	0.782	0.156	24.749	41.35	4400	48
2 1/4	0.906	0.219	30.944	33.07	3300	36
2 1/2	1.031	0.219	40.071	25.54	3300	36
2 3/4	1.156	0.219	50.377	20.31	2200	24
3	1.281	0.219	61.861	16.54	1650	18
3 1/4	1.375	0.250	71.273	14.36	1650	18
3 1/2	1.500	0.250	84.821	12.06	1190	13
3 3/4	1.625	0.250	99.546	10.28	1100	12
4	1.750	0.250	115.45	8.86	1100	12
4 1/4	1.875	0.250	132.53	7.72	1100	12
4 1/2	2.000	0.250	150.79	6.79	640	7

The shielding material is to be arranged in a cylindrical shape and will form the basic supporting structure as well as the transportation cask for the source material. The ends of the cylinder will be shielded by positioning end slabs of a configuration which will allow coolant to enter and leave the heater. Figures 3 and 4 show cross sectional views of the arrangement and give the nomenclature that will be used throughout the calculations.

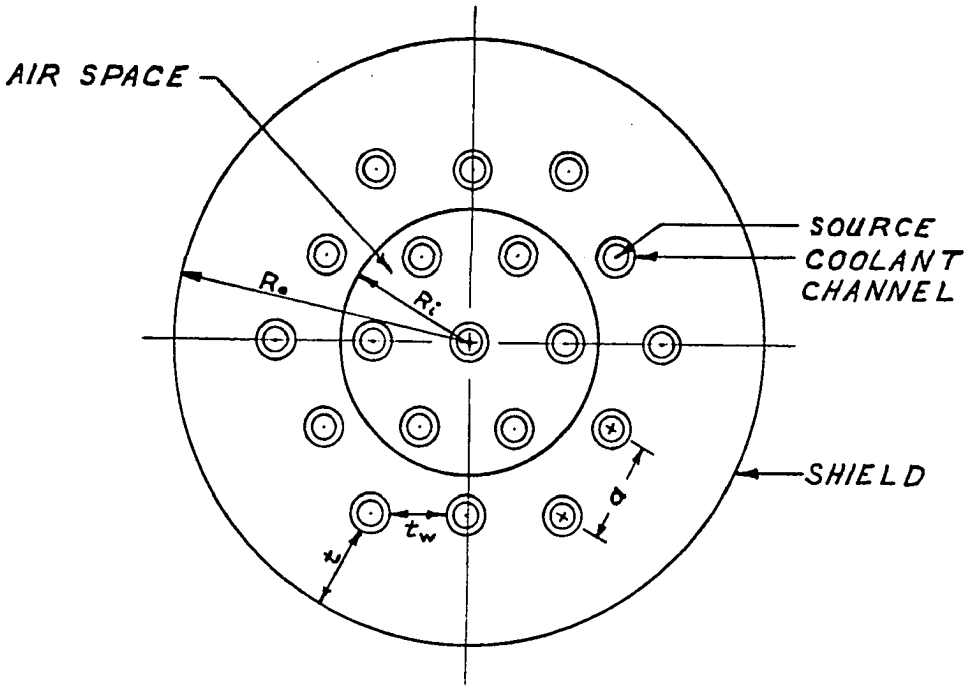

Figure 3. Cross section of fission-product heater

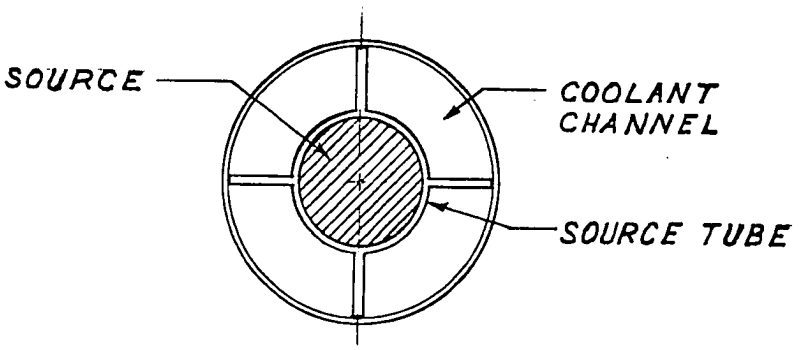

Figure 4. Cross section of source tube and coolant channel

Materials

The requirements for the materials used in this design are not beyond the present technology and most could be readily fabricated. The components of concern are:

1. Source tube material
2. Shield material
3. Shield cladding
4. Coolant tube material

Inasmuch as the calcined source material is an oxide and relatively inert, the prime consideration for the source tube material is resistance to temperature effects and corrosion for long periods of time. It would be quite unacceptable for the source tube to develop leaks through which radioactive material might escape. The material presently used for containers of calcined waste storage is schedule - 40 stainless steel pipe (20, p. 5, 17, pp. 12 - 13). Chance - Vought (12, pp. 41 - 43) recommended Hastelloy C due to its very low corrosion rate. Cost of the material will be but a small fraction of the total cost and is not considered a significant factor. Hastelloy C also has good weldability and has a melting point of 2300°F compared to 2600°F for stainless steel. Its corrosion rate in sea water is quoted as 0.000006 - 0.0001 inches per year while stainless steel is of the order of 0.001 inches per year. In addition stainless steel is subject to pitting and corrosion near the welds.

The shield material must have the properties of high density, ease of fabrication in the geometry required, and a high melting point. Depleted uranium is well suited to meet these requirements. Blockage of the coolant channels or ducts for extended periods of time might

result in temperatures near its melting point. As pointed out in reference (12, p. 104), proper cladding of the shield could make the heater practically fire proof since it would provide strength when the uranium softens near its melting point. The major disadvantage of uranium is its relatively high cost ($5.00 to $30.00 per pound for machine finished castings). The coolant tubes provide channels for the air flow along the tubes, positioning fixtures for the source tubes, and where they pierce the uranium shield they act as cladding for the shield.

Since all of these parts are in contact, consideration must be given to the compatibility of the materials in the environment in which they will be exposed as well as to the other features of fabrication. The following is a summary of the proposed materials used in this design.

1.	Source tube material	Hastelloy C or stainless steel
2.	Shield material	depleted uranium
3.	Shield cladding and coolant tubes	stainless steel

The pertinent properties are given in Table 10 and Figure 5.

Biological Shielding

The basic requirement of the shielding is that it attenuate the radiation so that the dose at the outside surface of the shield complies with ICC regulations, viz., 200 mr/hr. This will allow using the shield as the transportation cask and will facilitate in installation at

Table 10. Properties of the materials selected

Property	Hastelloy C (21)	304 Stainless steel (22)	Uranium (23)
Density (lb/in.^{3})	0.323 (72°F)	0.29 (70°F)	0.675
Melting point	2300°F	2600°F	2070°F
Weldability	any method - oxy-acetylene not recommended for corrosive service	good	inert gas techniques
Machinability	good - tungsten carbide bits recommended	poor	good
Formability	same as 300 series stainless steel	very good	good
Thermal conductivity (Btu/hr/ft/°F)	(see Figure 5)	(see Figure 5)	17.18 (158°F)
Corrosion resistance	very good for chlorides and most others	high resistance to corrosion by most materials	poor
Oxidation resistance in air	good up to 2000°F	good up to 1600°F continuously	poor
Coefficient of expansion (in./in.-°F)	6.3×10^{-6} (32 - 212°F) 8.5×10^{-6} (32 - 1800°F)	9.6×10^{-6} (32 - 212°F) 11.2×10^{-6} (32 - 1800°F)	variable - depends on fabrication - castings; 7.22 to 8.33×10^{-6}
Tensile strength	121,000 psi (70°F) 18,300 psi (2000°F)	87,000 psi (70°F) 5,500 psi (2000°F)	56,000 psi (70°F)

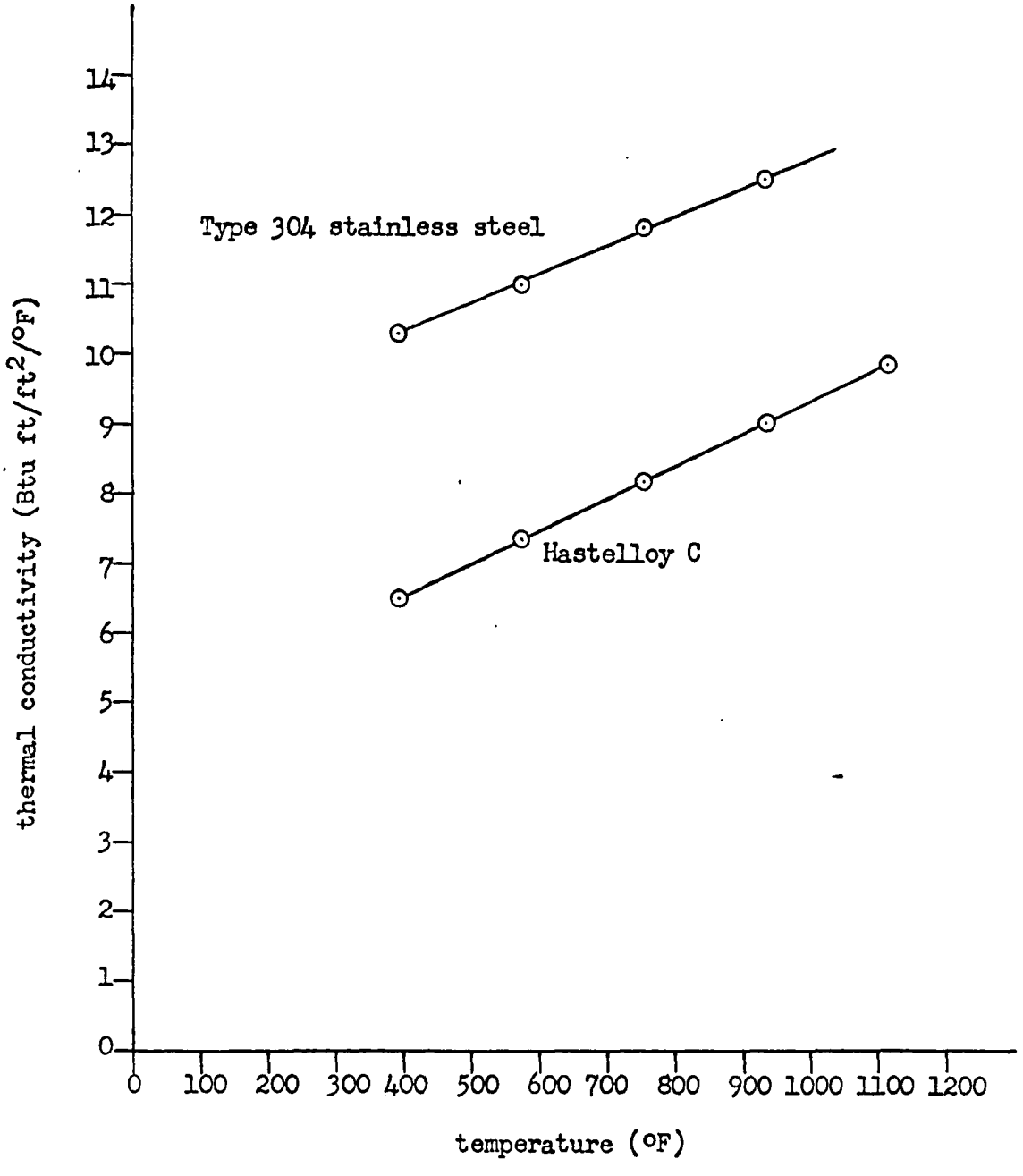

Figure 5. Thermal conductivity for Hastelloy C and 304 stainless steel

the site. At the outset it must also be recognized that the shield is likely to account for nearly all the weight and a large share of the cost, therefore any reduction in size is important.

An estimate of the shielding required can be obtained by assuming a uniform volume distributed source shielded by a slab of uranium. Because of the large inside radius of the shield the curvature will have little effect and one-dimensional calculations are adequate. One of the conventional methods for dealing with a shielding problem such as this is to use the line source approximation and consider self-shielding. The energy flux (Mev/sec/cm^2) at the outer surface of the shield can be evaluated by using the method given in reference (24, pp. 144 - 150). The results shown in Figure 6 were obtained by using the fission product data for decay times of 1, 3, and 30 years from Table 3 and assuming the mass absorption coefficient, μ_c, for the source material to be the same as that for aluminum (their densities are nearly equal - $\rho_{fp} = 2.4$ gm/cm^3 and $\rho_{Al} = 2.7$ gm/cm^3). Table 11 gives the values used for mass absorption coefficients (24, p. 104). The energy flux which is equivalent to the permissible dose in this case is

$$\phi_e 200\text{mr/hr} = \frac{(0.2 \text{ rem/hr})(100 \text{ erg/g-rad})}{(1.6 \times 10^{-6} \text{ erg/mev})(0.02509 \text{ cm}^2/\text{g}_{air})(3600 \text{ sec/hr})}$$

$$= 1.384 \times 10^5 \text{ mev/cm}^2\text{sec}$$

The required shield thickness is approximately 10 cm (4 inches).

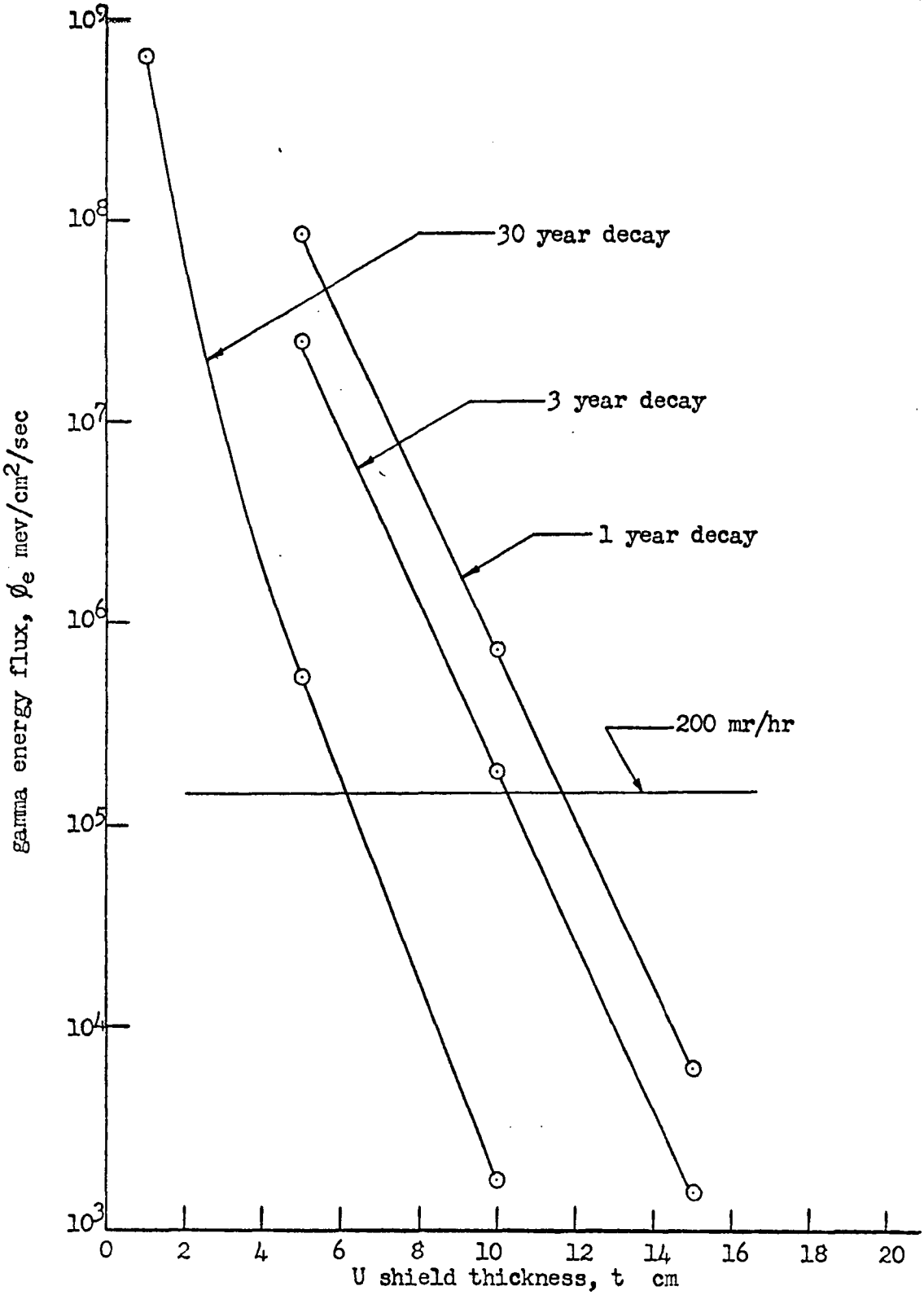

Figure 6. Approximate shield requirements for GFP

Table 11. Mass absorption coefficents

Gamma energy mev	Mass absorption coefficient for uranium cm^{-1}	Mass absorption coefficient for FP (Al) cm^{-1}
0.125	62.40	0.405
0.67	2.55	0.208
1.67	1.02	0.130
2.4	0.83	0.105

With this as a starting point more accurate calculations can be made. Consider three source rod sizes filled with source material which has decayed three years. Figures 7, 8, and 9 show a sector of each of these examples drawn to scale and in Table 12 the data are presented. There are several points worth noting before evaluating the shield for these examples. On the basis of reducing the shield weight (therefore the cost) it is desirable to put the source in as large a tube as possible and space the tubes as closely as possible. The limitation to increasing the size of the source tube is imposed by the heat transfer characteristics of the calcined material. It seems desirable to keep the maximum temperature within the source below the melting point and possibly below the calcination temperature (16). On the other hand further research may show that it is desirable and entirely safe to operate with molten source material.

Inasmuch as the shielding calculations are long, the best design from the stand point of minimum shield weight will be considered.

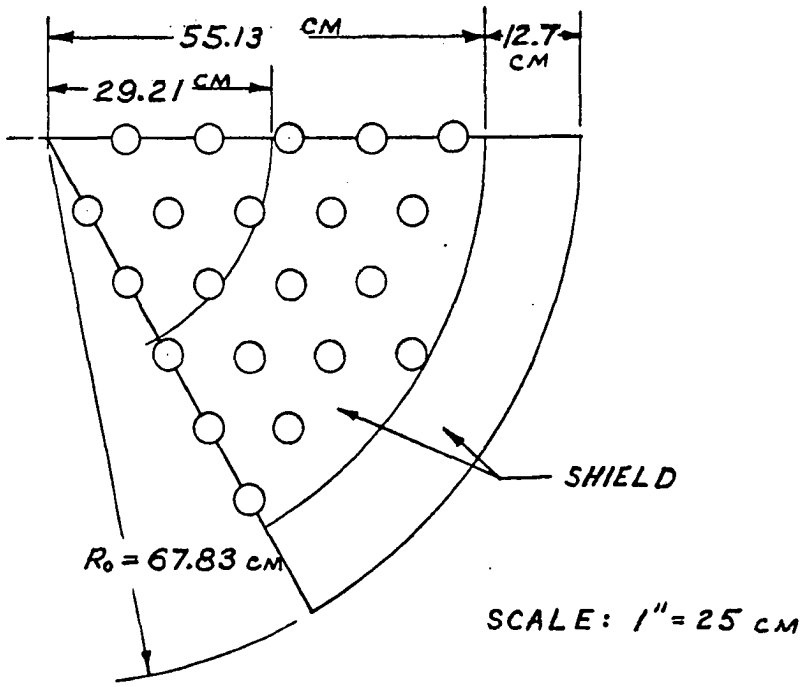

Figure 7. Sixty degree sector of heater using 1 3/8 inch diameter source tubes

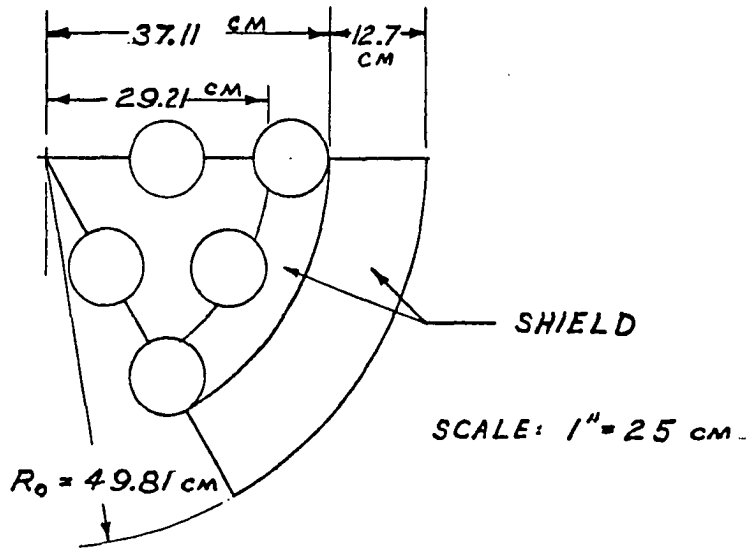

Figure 8. Sixty degree sector of heater using 3 inch diameter source tubes

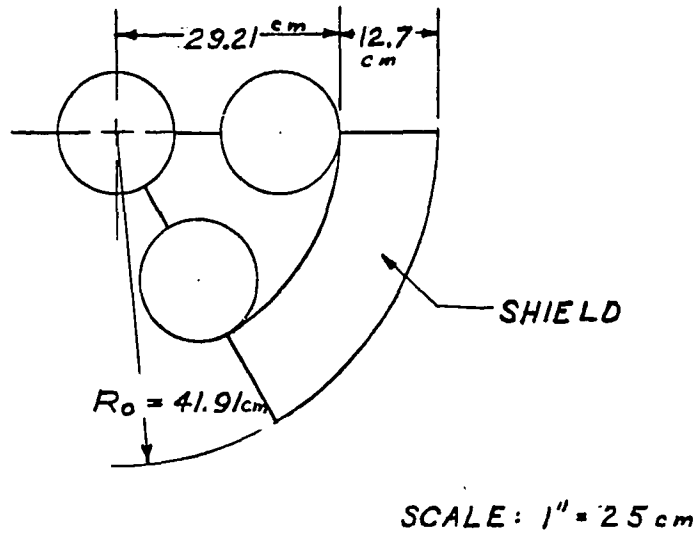

Figure 9. Sixty degree sector of heater using 4 1/2 inch diameter source tubes

Table 12. Calculated data of Figures 7, 8, 9, and 10

Figure	Source tube O.D. inches	Inside radius cm	Source spacing cm	Shield thick t cm	Shield thick t_w cm	Shield R_i cm	Shield R_o cm	Shield weight tons
7	1 3/8	1.35	10.409	12.7	6.35	29.21	67.83	22.40
8	3	3.26	16.115	12.7	6.35	29.21	49.81	9.71
9	4 1/2	5.08	21.590	12.7	6.35	29.21	41.91	5.38
10 (D)	4 1/2	5.08	17.020	12.7	0.00	25.50	38.20	4.82

The example of Figure 10 (point D) is a case of maximum source size (within previous assumptions) and minimum spacing. The results show a saving in shielding weight of over 10%. By considering each of the seven sources as independent volume distributed sources the energy-flux at point D on the surface radially opposite a source is 3.46×10^4 mev/cm^2/sec. The allowable value (for 200 mr/hr) is 1.384×10^5 mev/cm^2/sec. This calculation of the dose is considered to be on the safe side since attenuation other than that due to self absorption and the shield was ignored. However, these calculations assume that the buildup factor is 1.0.

Further calculations for a thinner (point E - 2.5 inches) and a thicker (point F - 7.5 inches) shield were completed and the results are presented in Figure 11. The tabulated results with calculated values for these examples are in the Appendix. Also shown in Figure 11 is the effect of including buildup factors. Reference to ANL - 5800

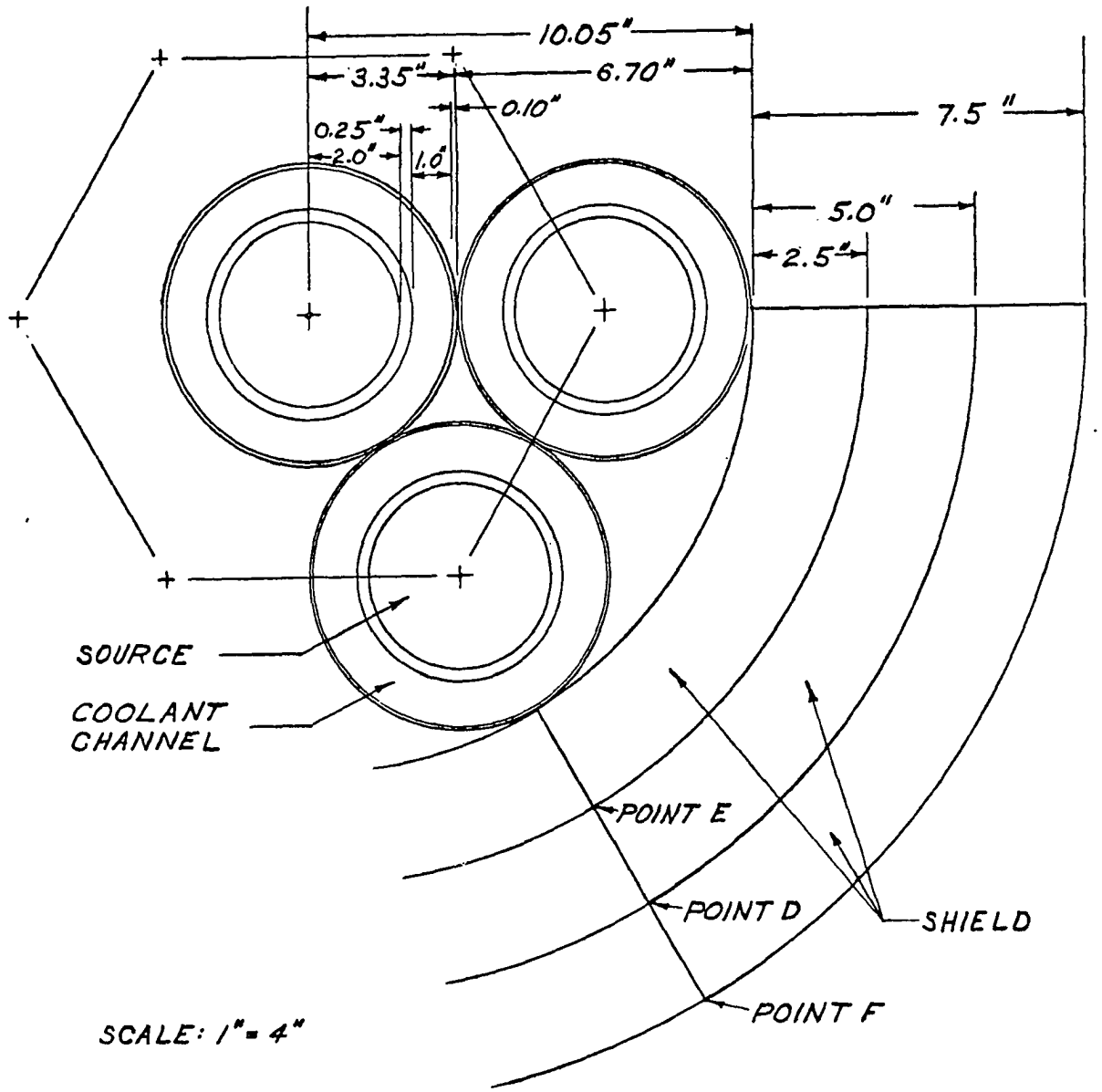

Figure 10. Minimum shield weight configuration, 4 1/2 - inch O.D. source tubes

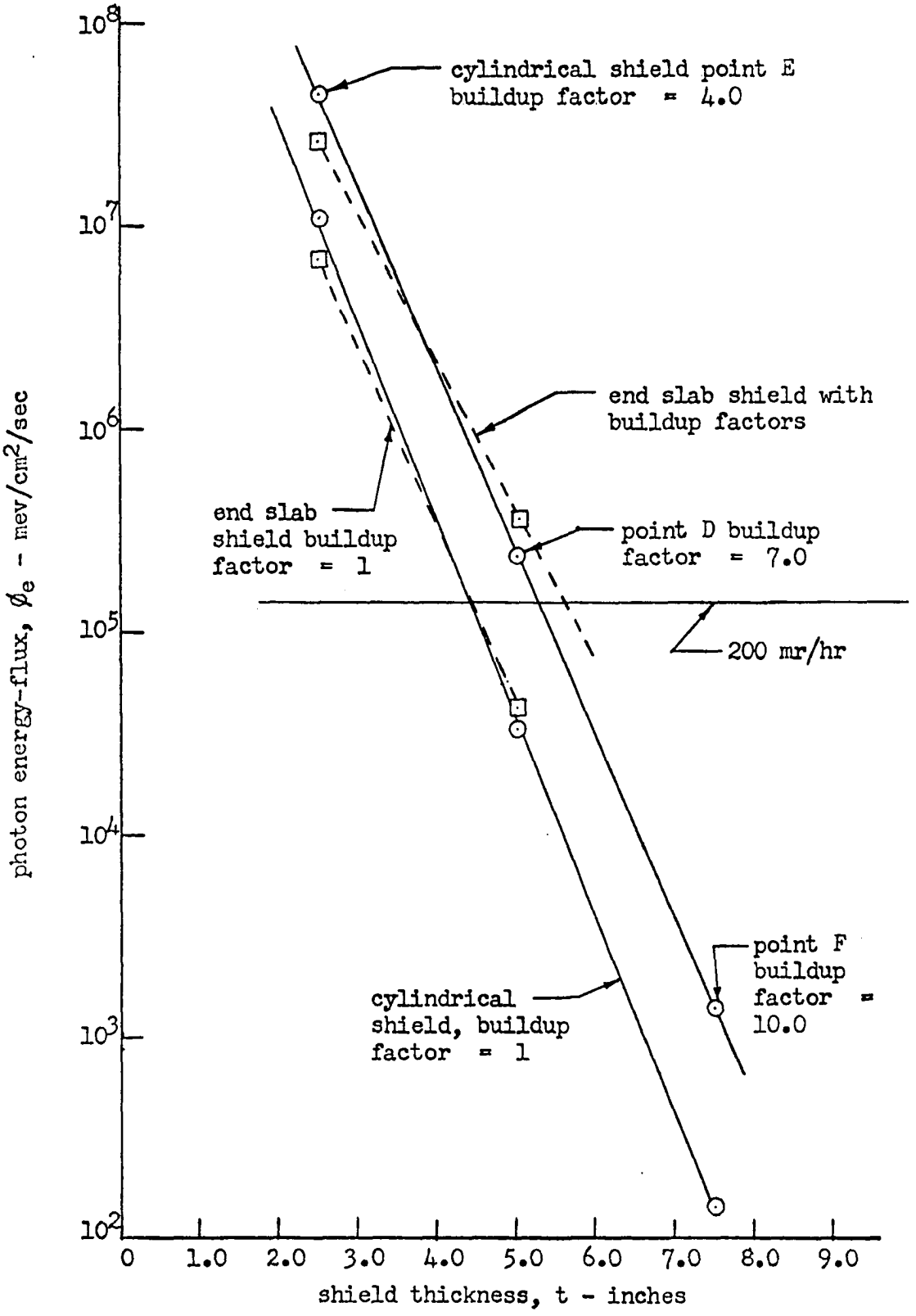

Figure 11. Photon energy-flux versus shield thickness

(25, p. 656) gives dose buildup factors for isotropic point sources. The group I (average energy = 0.125 mev) and group II (average energy = 0.67 mev) calculations for the 2.5 - inch and the 5.0 - inch shield show that these photons form a very small fraction of the total dose (maximum of 0.1%). In addition the buildup factor is very low for these energies. As a result these two groups have little effect and need not be considered for the examples even when buildup factors are included. The conclusions in Table 13 were reached by studying the calculated data and the buildup factor tables.

Table 13. Buildup factors

Shield thickness inches	Group	Maximum number relaxation lengths μt	Buildup factor
2.5	III	8.16	4.0
	IV	6.65	4.0
5.0	III	15.80	5.0
	IV	12.90	7.0
7.5	III	22.65	6.0
	IV	18.45	10.0

The curve in Figure 11, which shows the effect of including the buildup factors, was obtained by using a factor of 4.0 for the 2.5 - inch shield, a factor of 7.0 for the 5 - inch shield, and a factor of 10.0 for the 7.5 - inch shield.

The intersection of these two curves with the 200 mr/hr line gives the shield thickness required. The increase in shield weight considering the buildup factors is about one ton (4.4 - inch shield weighs about 4.17 tons and the 5.3 - inch shield weighs about 5.17 tons) or about a 24% increase in weight due to the buildup factors.

As a check on these calculations it is of interest to compare the shield thickness required for a point source of 50,000,000 curies, considering exponential buildup factors. The calculation used a modified computer program prepared by Moser (26). The results are summarized in Table 14. Reference to Table 8 shows there are nearly 10 times

Table 14. Uranium shield thickness for a 50 Mc point gamma source (surface dose = 200 mr/hr)

Photon energy mev	Shield thickness cm
0.5	7.35
1.0	16.88
2.0	26.68
3.0	30.97

as many photons below 1.0 mev as above for fission products. On this basis it might be argued that the 1.0 mev energy is representative of the fission products emission. The point source would also be expected to produce a higher shield requirement since self-shielding

and geometry factors are important. Comparing the 16.88 cm at 1.0 mev to the 13.4 cm gained by the previous calculation provides an approximate check.

The total weight of the shield for the heater must include the end slabs as well. If the source region is treated as a cylindrical volume source 25.5 cm in radius, the shield thickness required can be determined by using the procedure of reference (24, p. 144) for a slab shield at one end. Two values of the energy flux were calculated with shield thicknesses of 2.5 inches and 5.0 inches (tabulated results are in Appendix). The results with a unity buildup factor and with a value of 4.0 and 7.0 for the two shields, as before, are represented on Figure 11 also. The intersection with the 200 mr/hr line occurs at about 5.55 inches. This value should also be on the safe side since it was assumed by the calculation that the source was in contact with the shield. If a 6 - inch space is left above and below the source tubes for coolant flow, the overall height of the shield is about 59.1 inches and the O.D. is about 30.7 inches. The total weight is estimated to be 9.3 tons. The overall dimensions are shown in Figure 12.

Heat Transfer and Fluid Flow

The primary objective of this fission-product heater is to produce no less than 25,000 Btu/hr over a period of 30 years. This energy is to be transferred to air flowing past the source tubes. The next step in this design is to calculate the factors controlled by the heat transfer and coolant flow to be sure they fall within acceptable limits.

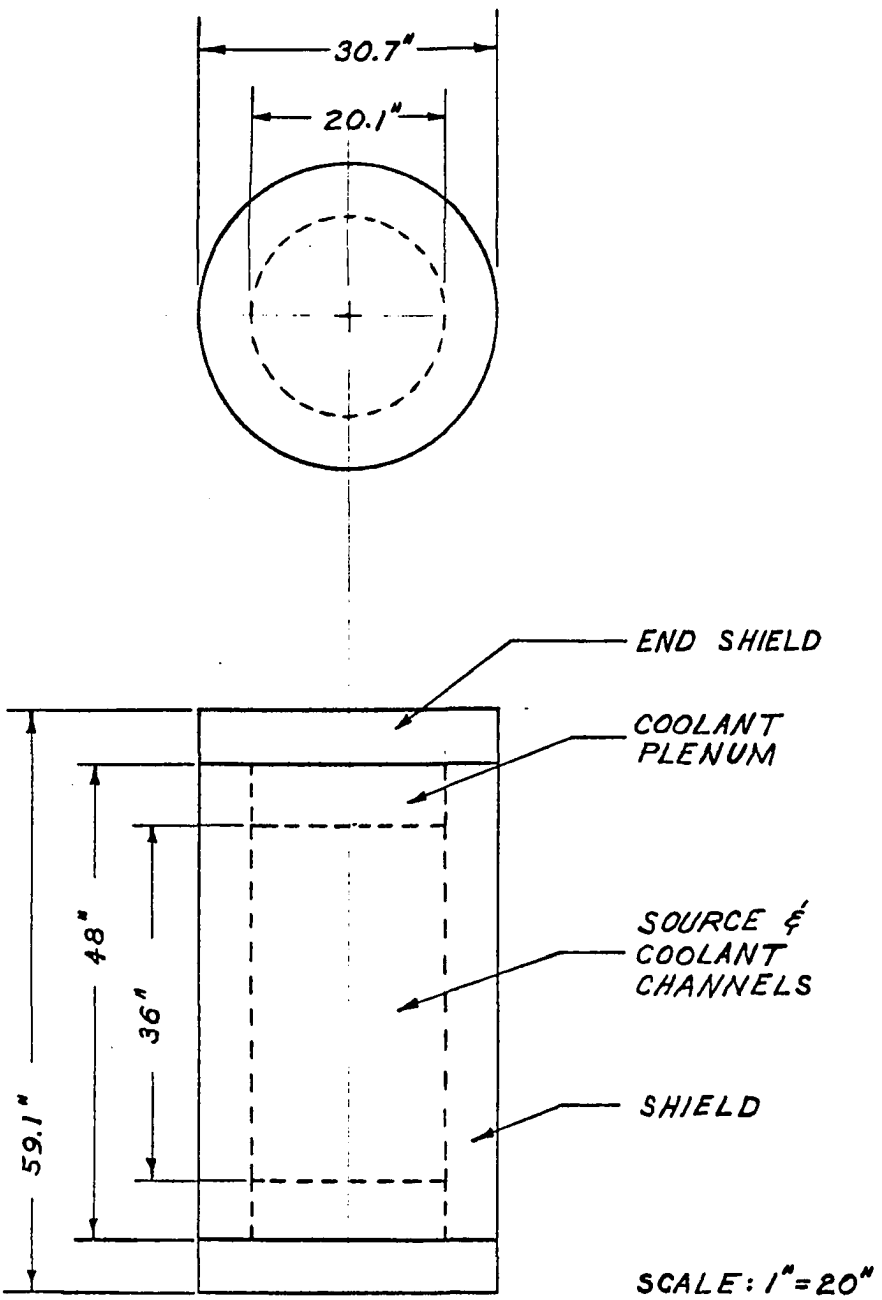

Figure 12. Overall dimensions of fission-product heater

Since the melting point of the calcined material is approximately 1000°C (1800°F), this temperature will be assumed as the limiting value. Reference to Glasstone and Sesonske (27, p. 358) provides the necessary heat transfer equations. If all of the energy is released within the source material and the conductivity, k, of the source material is equal to 0.5 Btu/hr/ft^2/°F (see Table 4), the temperature at a point on the surface of the source material is

$$T_1 = T_o - \frac{Qr^2}{4k} = 1800 - \frac{(32.35)(2.0)^2(12)}{(4)(0.5)} = 1024^\circ F$$

where T_1 and T_o are the temperatures at the indicated points of Figure 13. Referring to Figure 5 for the thermal conductivity value, k_c, the temperature drop across the Hastelloy C cladding is

$$T_2 = T_1 - \left(\frac{Qr^2}{2k_c}\right) Ln\left(\frac{r_1}{r_2}\right) = 1024 - \frac{(32.35)(2)(12)}{(2)(9.29)} Ln\left(\frac{2.250}{2.000}\right)$$

$$= 926^\circ F.$$

If the air (coolant) enters at 70°F and leaves the heater at 300°F, the mass rate of flow of the coolant, W, will be about

$$W = \frac{Q_t}{C_p\,(T_o - T_1)} = \frac{(30)(3413)}{(0.24)(230)} = 1855 \text{ lb/hr}$$

where Q_t is the total output of the heater and C_p is the specific heat of air at constant pressure. The resulting Reynolds number (N_{re}) is

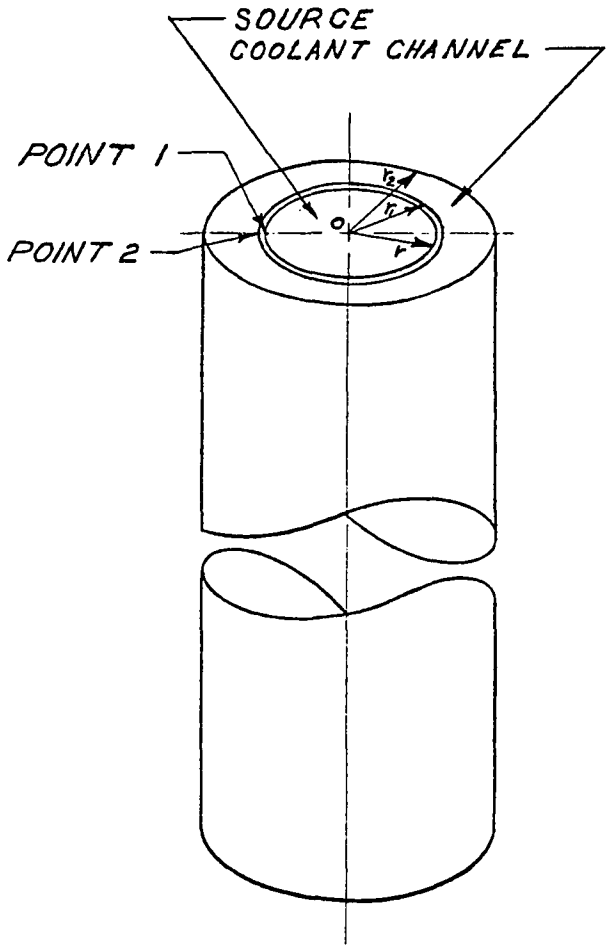

Data

No. of tubes = 7

Annulus area = 17.3 $in.^2$

Source area = 12.58 $in.^2$

Source vol/tube = 452.5 $in.^3$

Total heat transferred/tube = 14,620 Btu/hr

Volume heat source, Q = 32.35 $Btu/in.^3$

r = 2.000 inches

r_1 = 2.250

r_2 = 3.250

Figure 13. Source and coolant channel for heat transfer and coolant flow calculations

$$N_{re} = \frac{\rho V D_e}{\mu} = \frac{(0.0617)(32{,}000)(2.0)}{(12)(0.051)} = 6450$$

where D_e is the equivalent diameter of the annulus without fins and the density, ρ, and viscosity, μ, are evaluated at the mean temperature of 185 °F. This N_{re} indicates the flow is in the laminar region or nearly so. By assuming the average coolant temperature is 300°F (a conservative assumption), the required convective heat transfer coefficient, h, is found by solving the equation

$$T_2 - T_m = \frac{Qr^2}{2hr_1}$$

for h. Evaluation gives

$$h = \frac{(32.35)(2)^2(144)}{(2)(2.25)(926 - 300)} = 6.6 \text{ Btu/hr/ft}^2/^\circ\text{F}.$$

A heat transfer coefficient of 6.6 Btu/hr/ft^2/°F is too high to expect from laminar flow as shown in the following calculations. Kreith (28, pp. 390 - 393) suggests that the Nusselt number (N_{nu}) can be calculated from

$$N_{nu} = 4.36 + \frac{(0.036)(N_{re}N_{pr}D/L)}{1 + (0.0011)(N_{re}N_{pr}D/L)}.$$

He also gives a correction for temperature effects on properties of the material as

$$N_{nu(corr)} = N_{nu} (T_b/T_s)^n$$

where T_b and T_s are the temperatures of the bulk stream and the surface, respectively. The value for n is given as 0.25 for a system heating a gas with a constant heat input and well-developed velocity profiles. Therefore, if

N_{re} = 6450 and

N_{pr} = 0.703 for air at 300°F, then

N_{nu} = 11.46 and

$$N_{nu(corr)} = (11.46) \left(\frac{300}{926}\right)^{0.25} = 8.92$$

Evaluating the coolant properties at the mean temperature of 185°F, the thermal conductivity of the air, k_a, is equal to 0.0174 Btu/hr/ft/°F. Then

$$N_{nu(corr)} = \frac{hD}{k} \text{ gives}$$

$$h = \frac{kN_{nu(corr)}}{D} = 0.931 \text{ Btu/hr/ft}^2/^\circ\text{F}.$$

It is obvious that laminar flow with this geometry is not satisfactory. There are at least three things which might be done to improve the heat transfer:

1. increase the Reynolds number,
2. install turbulence-promoters in the flow channel, or
3. add fins to the source tubes.

The third possibility is the most inviting since the laminar flow condition with its low system pressure drop will be maintained. Another reason for designing for laminar flow is that under emergency operation (no fans) the heater will be adequately cooled by natural convection. If economy of pumping power is to be of interest, smooth, longitudinal fins will probably give the best results (29, pp. 85 - 91).

Obert and Young (30, p. 441) discuss the time rate of heat transfer by extended surfaces such as fins. Figure 14 gives the nomenclature.

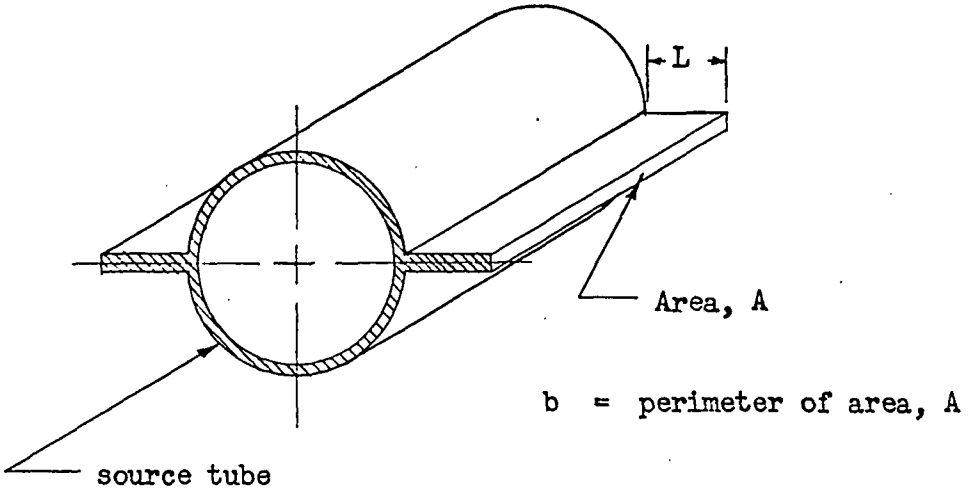

Figure 14. Finned tube nomenclature

The heat transferred by an integral fin, Q_f, is

$$Q_f = k_c A (T_2 - T_m) a \tanh (aL)$$

where

$$a^2 = \frac{hb}{k_c A}$$

if

h	= 1.0 Btu/hr/ft^2/^{o}F	Fin thickness	= 0.1 inches
L	= 1.00 inch	T_2	= 926 ^{o}F
b	= 72.2 inches	T_m	= 300 ^{o}F
A	= 3.6 inches^2	k_c	= 9.29 Btu/hr/ft/^{o}F

The heat transferred per hour per fin is 355 Btu. The total heat to be transferred by the tube is 14,620 Btu/hr and the number of fins required is 4.125. There are a number of approximations made to arrive at this number but it seems clear that relatively few fins on the tubes will make the design feasible. Calculations of heat transfer in the longitudinally finned coolant channels of the Windscale reactor, which were based on comparing the finned channel with a tube of the same effective diameter, predicted a heat transfer coefficient that was about 30% low. This, however, was a case of turbulent flow with more closely spaced fins (29). For ease of spacing, six fins per tube will be used in this design.

A more refined calculation can now be made as a check on the previous calculations for an annulus. Figure 15 shows the source tube and coolant channel cross section drawn to scale.

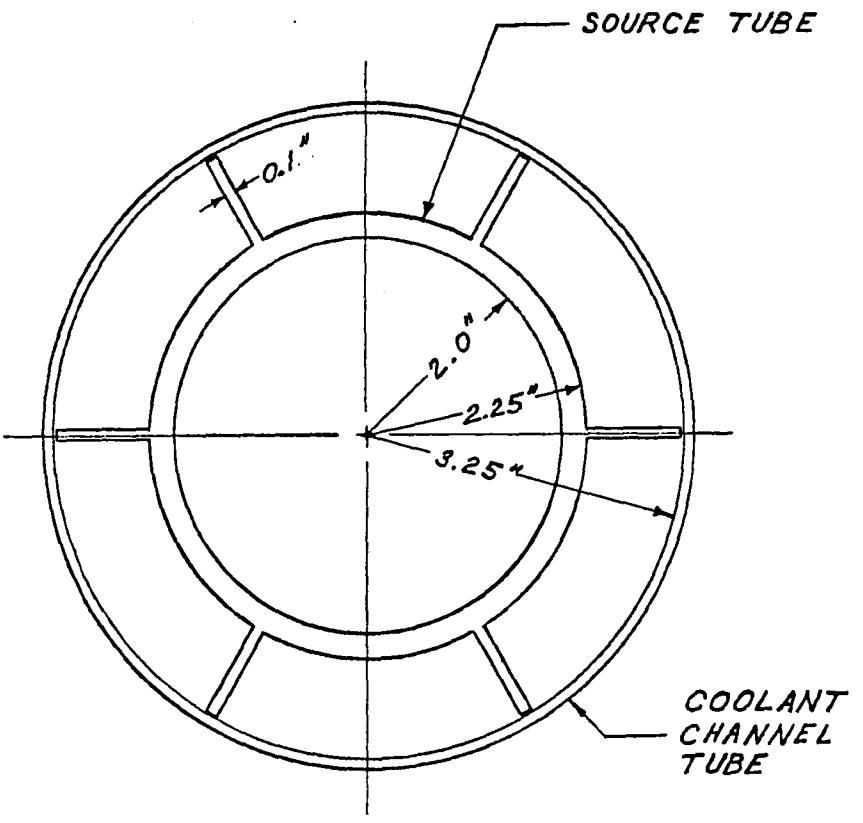

Figure 15. Source tube and coolant channel cross section

If the spaces between the fins are assumed to be coolant channels, the flow area per channel is 2.775 $in.^2$. This results in a velocity of 33,200 ft/hr. With an equivalent diameter of 1.469 inches, the Reynolds number for the channel becomes 6,010. A value of 9.57 is obtained for the Nusselt number by using the relation given by Kreith, and the value for $N_{nu(corr)}$ becomes 7.22. The heat transfer coefficient is found to be 0.943 $Btu/hr/ft^2/^oF$.

A further check on the validity may be obtained by use of other correlations such as those of McAdams (31, p. 173) and Jakob (32, pp. 529 - 530). McAdams gives the following simplified expression for air at ordinary pressures and temperatures for vertical surfaces:

$$h = 0.19 (T_2 - T_m)^{0.333}$$

The heat transfer coefficient is found to be 1.62 $Btu/hr/ft^2/^oF$. Jakob suggests using the following:

$N_{nu} = 0.129 (N_{gr} N_{pr})^{0.333}$ where N_{gr} is the Grashof number.

In this example, $N_{gr} = 4.8 \times 10^9$ and $N_{nu} = 193.5$. When the length of the channel is used as the characteristic length, the heat transfer coefficient is found to be 1.032 $Btu/hr/ft^2/^oF$.

In conclusion it appears that a design value for the convective heat transfer coefficient of 1.0 $Btu/hr/ft^2/^oF$ is a reasonable value. Under operating conditions, it may be too low since the flow is near if not in the turbulent region. If emergency conditions arise where the fans are inoperative and natural convection chimney effect must

be relied upon to cool the source rods, the value of 1.0 for h is probably quite realistic. Should there be a need for more heat transfer area, it would be a relatively simple matter to increase the number of fins on each tube. Because of emergency operation requirements it would probably be undesirable to use a large number of longitudinal fins or transverse fins. In any event sources much larger than four inches in diameter will probably develop high center line temperatures. If temperature becomes a problem, it might be reduced by incorporating radial heat paths of relatively good conducting material within the calcined source.

Gamma Ray Heating

This part of the design calculation is concerned with the energy deposited in the shield as the result of attenuation of the photons produced in the source material. The total energy deposited in the shield has already been determined in effect since the total energy release rate of the source is known and the shield thickness was calculated by assuming the permissible energy escape. However, calculation of the total energy deposited is not the objective, but rather the determination of the energy deposited at a particular location and the resulting localized maximum temperature. The limitation on the temperature rise for uranium is the temperature at which the alpha phase changes to the beta phase. This occurs at 1230 ^{o}F (27, pp. 466 - 469). It may be desirable to use a stabilized alloy of uranium

if the temperature rise is too great. In that case, either thermal expansion or the melting point temperature of the alloy could be the limitation.

The geometry of the general design for any size source rod from a radius of 0.532 inches to 2.00 inches presents a rather severe complication to heat transfer calculations. In general one can visualize 3 separate regions to be considered. Referring to Figure 16, region A consists of source tubes surrounded by coolant channels but no intervening shield material, region B is made of the same source and coolant channels but the coolant channels are surrounded by shield material, and region C consists of shield material only. The following assumptions are made:

1. Radiation will be attenuated exponentially in regions B and C as though B was solid material.
2. The gamma flux at any point within the shield is a summation of the exponentials from all sources.
3. The energy given up in the attenuation process will appear as heat with the same distribution (i.e., exponential) since the interactions are with electrons and they travel short distances in a heavy material like uranium.
4. The exterior of the shield is insulated to prevent the escape of heat to the environment.
5. The A-B interface is cooled to a maximum temperature of 300 °F.

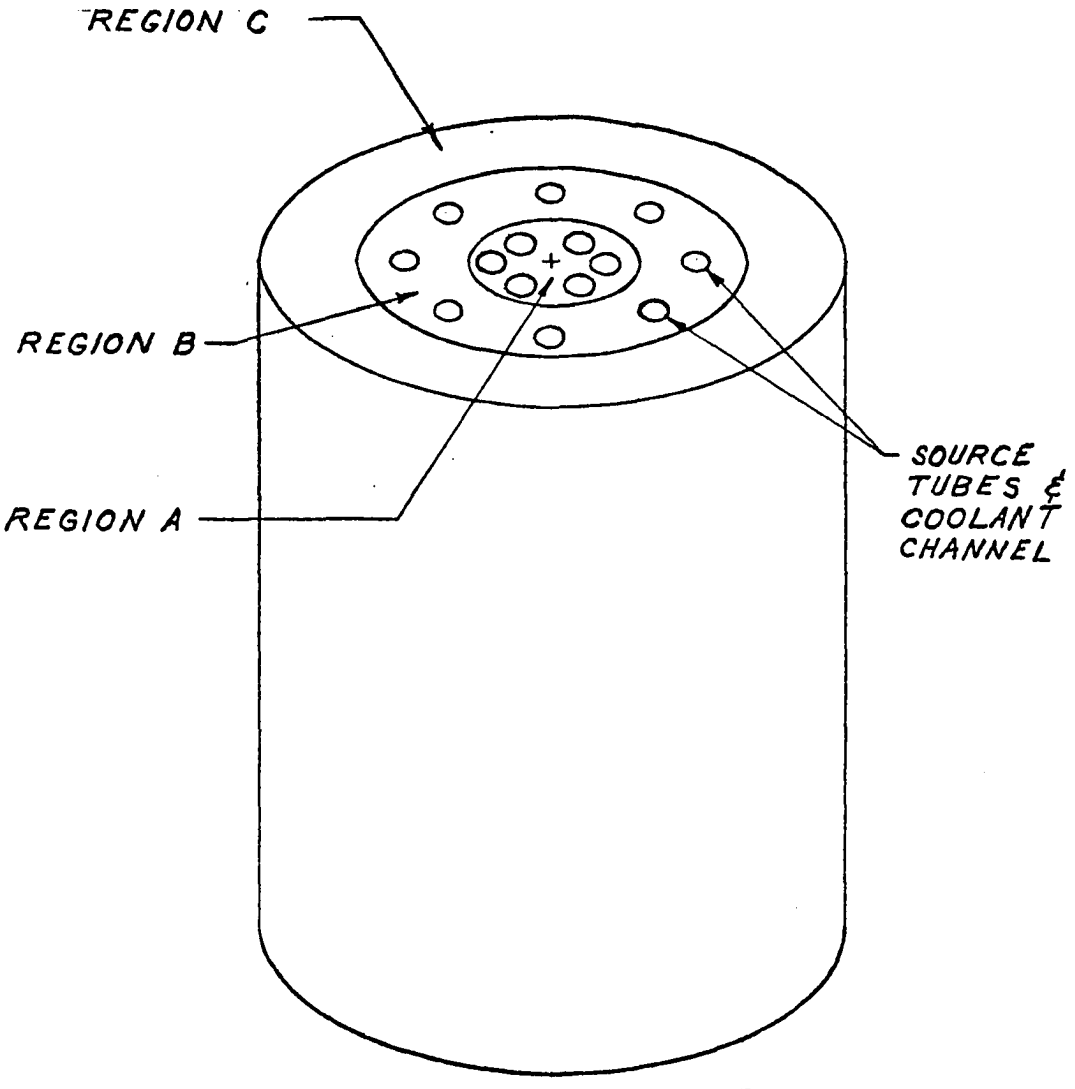

Figure 16. Heater regions for general gamma ray heating calculations

The design which has been used up to this point, viz., the source rod radius equal to 2.00 inches, allows considerable simplification since there are only two areas to be considered and relatively few sources. Each source will be treated individually as a volume distributed source. Self shielding will be considered but the effect of the source tubes, fins, and shield cladding will be ignored in the calculations made to determine the energy flux at radial points from the inside of the shield to its outer surface. The shielding effect of an intervening source rod will also be ignored. All of these factors which are to be ignored should be on the conservative side from a safety point of view.

Since prediction of the maximum temperature in the shield and approximately where it will occur is of interest, a radial cutting plane through the center lines of three of the sources will be considered (EDF plane of Figure 10). The calculations will be made for the horizontal midplane of the heater. The energy per unit volume per unit time is calculated from the following expression (27, p. 616):

$Q_z = B_e \mu_e \phi_e$ where

Q_z = mev/cm^3/sec

B_e = energy absorption buildup factor

μ_e = energy absorption coefficient - cm^{-1}

ϕ_e = photon energy flux at the point considered - mev/cm^2/sec.

The values of μ_e were obtained by interpolating the data from ANL-5800 (25, p. 655). Table 15 gives the values for the four energy groups considered in this design.

Table 15. Energy absorption coefficients

Photon group	Photon energy mev	μ_e cm^{-1}
I	0.125	78.7
II	0.67	1.52
III	1.6	0.63
IV	2.4	0.605

The values for the energy flux for the four groups have already been calculated for the locations D, E, and F of Figure 10. The first step will be to determine ϕ_e values for points along the heater radius close to the inside surface. The points to be used, starting from the inside of the shield with z = 0, will be 0.0, 0.1, 0.2, 0.5, 1.0, and the last point, E, at z = 6.35 cm. Source material which has decayed for a period of three years will be used as before. The results of these calculations are shown in Figure 17 and the tabulated calculations are given in the Appendix. These results include buildup factors as given by ANL-5800 (25, p. 656).

As was indicated before, the heat transfer calculations can be greatly simplified by assuming the outside surface of the shield to be perfectly insulated. Further simplifying assumptions are permitted because shield temperatures are restricted to values below a specified maximum. The heat transfer model will substitute an arbitrary but conservative stair step approximation for the energy deposition rate

versus thickness curve as shown on Figure 17 by the dotted line. Note that the highest energy deposition rate is fortunately nearest the coolant (region A).

The shield is divided as indicated in Figure 18. The energy is transferred by conduction to the inside surface of the shield which is assumed to be cooled only by natural convection. The maximum temperature at the interface of the shield and its insulation can be determined. The following example calculations will show the method and the results are tabulated in Table 16. The conduction equation for a steady state system with an internal source is

$$Q_z = - k \frac{d^2 t}{d Z^2}$$

where Q_z is the volumetric source strength. The boundary conditions are $Z = 0$, when $t = t_o$ and $Z = Z_1$ when $t = t_1$. The solution is

$$t = - \frac{QZ^2}{2k} + \left(\frac{t_1 - t_o}{Z_1} + \frac{QZ_1}{2k} \right) Z + t_o$$

$$\frac{dt}{dZ} = - \frac{QZ}{k} + \left(\frac{t_1 - t_o}{Z_1} + \frac{QZ}{2k} \right)$$

$$q = - k A \frac{dt}{dZ}$$

$$\text{so } q/A = - k \frac{dt}{dZ}$$

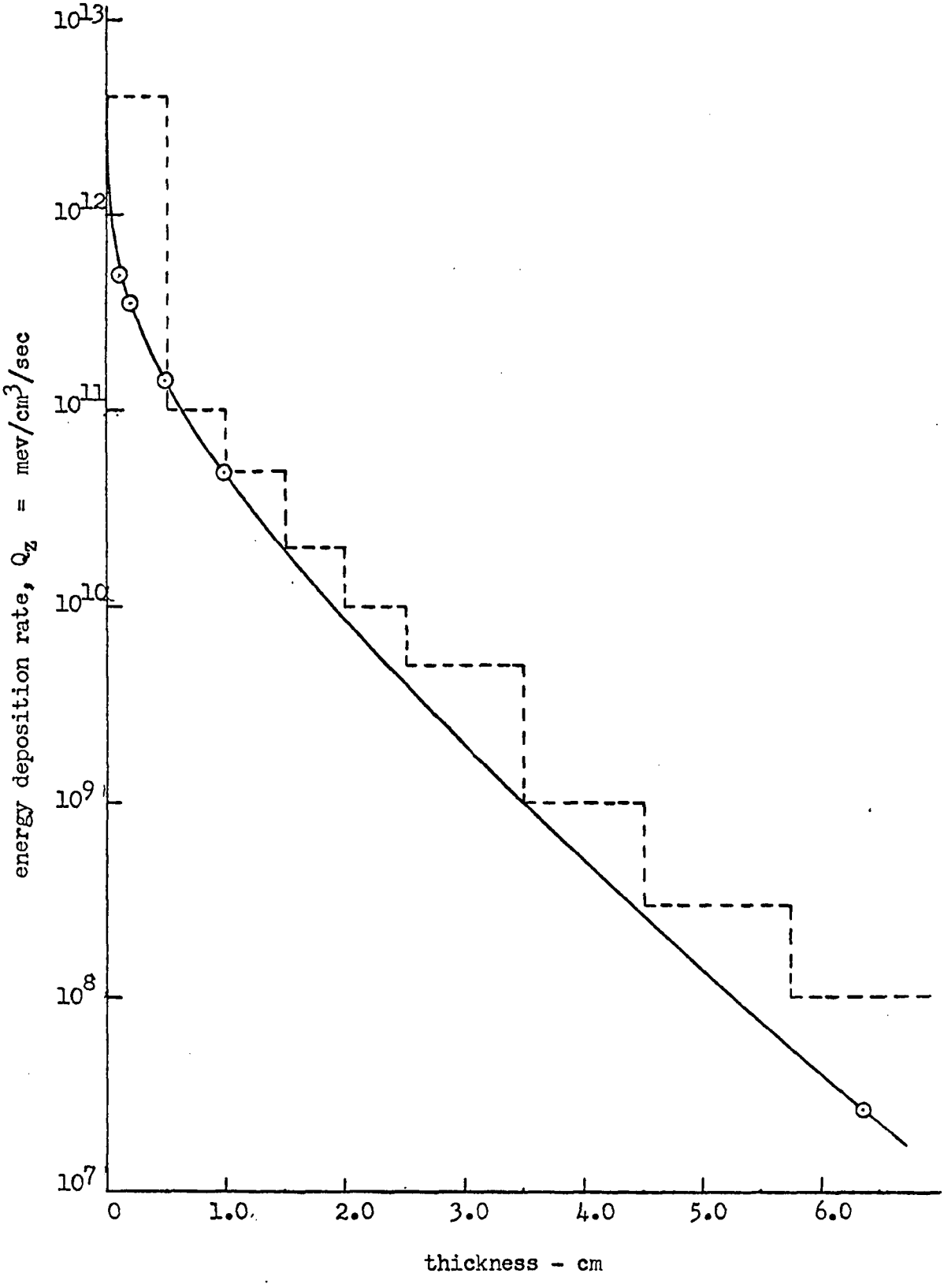

Figure 17. Photon energy deposition rate versus shield depth

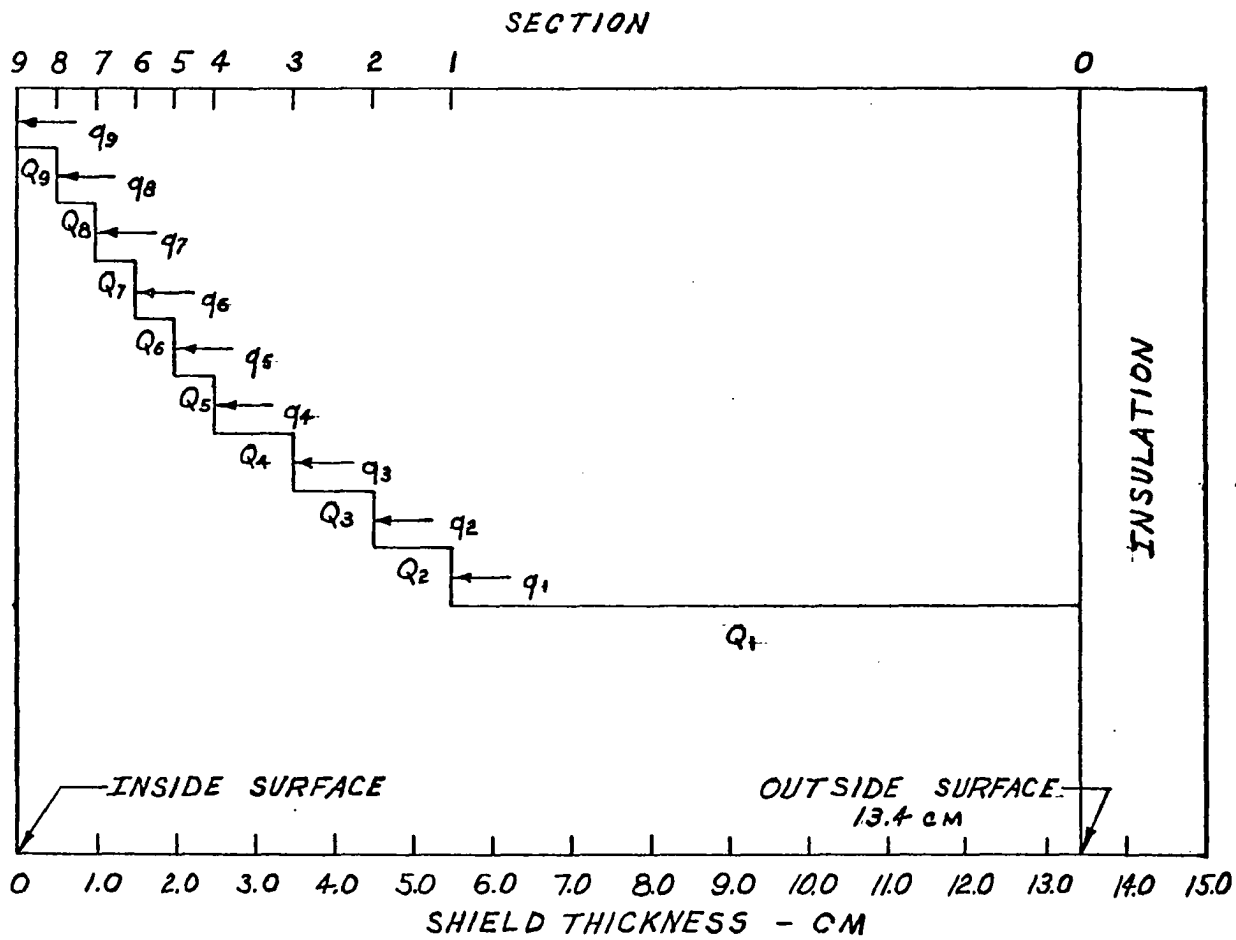

Figure 18. Shield divisions for gamma ray heating calculations

where q is the energy conducted out of a section. The energy conducted out of section (0 - 1) is equal to the heat generated in the section under steady state conditions.

Table 16. Incremental temperature difference data for gamma heating calculations (Figure 18)

Section	Q_{z_z} mev/cm^{3}sec	Q_z Btu/hr/ft^3	ΔZ cm	ΔZ in.	Δt °F	q/A Btu/hr/ft^2
0 - 1	$1X10^8$	1.55	7.9	3.110	0.004	0.40
1 - 2	$3X10^8$	4.65	1.0	0.394	0.001	0.56
2 - 3	$1X10^9$	15.5	1.0	0.394	0.002	1.06
3 - 4	$5X10^9$	77.5	1.0	0.394	0.005	3.60
4 - 5	$1X10^{10}$	155.0	0.5	0.197	0.006	6.14
5 - 6	$2X10^{10}$	310	0.5	0.197	0.010	11.22
6 - 7	$5X10^{10}$	775	0.5	0.197	0.020	23.92
7 - 8	$1X10^{11}$	1550	0.5	0.197	0.043	49.32
8 - 9	$4X10^{12}$	62000	0.5	0.197	0.584	1067
			Total T =		0.675 °F	

$$q_1/A = Q Z_1 - (t_1 - t_o) \frac{k}{Z} - \frac{QZ_1}{2} \quad \text{and}$$

$$q_1/A = Q_1 Z_1 \quad \text{so}$$

$$t_o - t_1 = \frac{QZ_1^2}{2k} \quad .$$

The heat conducted out of section (1 - 2) is equal to the heat conducted into the section from the adjacent one plus the heat generated within the section under steady state conditions. Applying the new boundary conditions, the resulting expression is

$$t_1 - t_2 = \left[Q_1 Z_1 + Q_2 (Z_2 - Z_1) - Q_2 Z_2 + \frac{Q_2}{2} (Z_2 + Z_1)\right] \frac{Z_2 - Z_1}{k}$$

and by analogy

$$t_2 - t_3 = \left[Q_1 Z_1 + Q_2(Z_2 - Z_1) + Q_3(Z_3 - Z_2) - Q_3 Z_3 + \frac{Q_3}{2}(Z_3 + Z_2)\right] \frac{Z_3 - Z_2}{k}$$

$$= \left[q_2 + Q_3(Z_3 - Z_2) - Q_3 Z_3 + \frac{Q_3}{2} (Z_3 + Z_2)\right] \frac{Z_3 - Z_2}{k} \quad .$$

In general

$$t_i - t_{i+1} = \left[q_i + Q_{i+1}(Z_{i+1} - Z_i) - Q_{i+1} Z_{i+1} + \frac{Q_{i+1}}{2}(Z_{i+1} + Z_i)\right] \frac{Z_{i+1} - Z_i}{k}$$

where $1 \leq i \leq 9$. By using the convection equation

$$q_9 = hA\,(t_9 - t_g)$$

and combining all expressions for temperature differences, the result is

$$(t_o - t_1) + (t_1 - t_2) + \ldots\ldots\ldots\ldots + (t_9 - t_g) = t_o - t_g \, .$$

If the convective heat transfer coefficient is 1.0 Btu/hr/ft^2/^{o}F,

$$t_9 - t_g = 1067\ ^oF \quad \text{and} \quad t_o - t_g \quad 1068\ ^oF.$$

If the temperature within region A is 300 °F the temperature of the outside surface of the shield is found to be 1367 °F. For normal operation the value of h = 1.0 is conservative for the space outside of the tubes. If the space becomes small (as it does in places) the natural convection currents will be suppressed and heat will be transferred by conduction. The temperature difference between the surface and the enclosed air for that case can be estimated by evaluating

$$q_9/A = \frac{k_A (t_9 - t_g)}{x}$$

where k_A is the thermal conductivity of air at temperature, t_g, and x is the thickness of the air space.

k_A = 0.0304 Btu/hr/ft/°F at 300 °F (31, p. 457).

If x is 0.25 inches $t_9 - t_g$ = 730 °F, on the other hand if x is 0.5 inches the temperature difference is 1460 °F.

The actual mechanism is probably a combination of convection and conduction and calculation is complicated by the irregular shapes between the cylinders. However, the melting point of the shield should not be exceeded and possibly not even the transition temperature of 1230 °F.

In conclusion it appears that gamma heating deep within the shield will not be a great problem. It is likely that no special coolant channels for the shield will be necessary. If a design is selected wherein some or all of the source rods pierce the shield these will

provide sufficient cooling for the shield. Should cooling of the shield surface be desirable it will be a relatively easy matter to provide region A with a small coolant flow. This air would be mixed with that going through the regular coolant channels.

SAFETY

Throughout the life of a device such as this fission product heater the overriding point of concern is for the safety of the personnel. The greatest hazards probably exist during fabrication of the source rods and transportation of the heater to the site where it is to be used. Once in place, routine maintenance will be slight and consist primarily of checking the warning devices. Of course there is the possibility of a loss of power for the cooling fans or a blocked passageway. The possibility of a fire or other catastrophe cannot be overlooked either.

The first of these areas, fabrication, is presently being accomplished at several Atomic Energy Commission installations where megacurie sources are regularly handled safely. The fact that this technology exists was the motivation for choosing cylindrical source rods.

The greatest potential hazard is expected to exist during transportation. Considerable care will be necessary during shipment to prevent an accident leading to large dose exposures of personnel in the area. The shield design was based on the limiting requirement of the Interstate Commerce Commission of 200 mr/hr at any accessible surface. If the shield is of sufficient thickness to satisfy the requirements and is further built to maintain its integrity in a collision or fire it will probably be a good transportation cask. If drop testing and fire testing prove that too much special construction is necessary, it may be desirable to construct a special frame to support the shield and sources during transportation.

In the case of a reusable shipping frame, there would be a number of advantages which might outweigh or cancel the additional cost and inconvenience of the frame. Once the source rods are in place they should be provided with a continuous supply of coolant. Making the fan an integral part of the heater design (in the case of no frame) will make the fan more costly and make maintenance of it more difficult once the heater is assembled and in place. If the fan was a part of the frame, the size and specifications could be fit to the space and power supply available on the carrier (rail, aircraft, etc.). The site of the installation could be provided with its fan installation independent of the frame and in such a location that routine fan maintenance could be easily done without radiation hazard. Another advantage to be gained by using a shipping frame is a decrease in the cost of the shield at the installation. This results from arrangements to eliminate the bottom end slab and use the earth or concrete.

If maximum protability is to be maintained, it is necessary that the shield and fan be integral and designed to withstand any conceivable fire or collision. Cladding the shield with stainless steel will probably give sufficient high temperature strength to keep the uranium shield in place during a fire. In any event a full scale mock-up with simulated source material in place will be required for collision and fire testing.

Under normal operation the only requirements for safe operation are those assuring that the monitoring and safety devices are working properly and that the waste heat is being disposed. Continuous

monitoring of the coolant stream for the presence of radioactive fission products will be desirable if not required. These monitors could be used to actuate warnings and divert the coolant flow through filters and vents. In addition a program of leak testing and periodic inspection of the source elements may be desirable. The requirement of 25,000 Btu/hr as a minimum at the end of a 30 - year period means there will be excess energy which must be used or dumped. At the beginning of the 30 - year period the heater will produce about 100,000 Btu/hr or four times the requirement. There will undoubtedly be times when the heat supply will not be needed or at least it will be desirable to "shut it off". To accomplish this kind of control will require a system which can divert the coolant stream and dump the energy to a sink such as the atmosphere. The arrangement which permits dumping the energy probably would be incorporated in provisions for the emergency operation.

There are two possible situations to be considered when emergency conditions exist.

1. Operation when the fan is inoperative but where natural circulation is available to cool the heater.
2. Operation with no coolant flow (blocked duct work).

The first situation might arise as the result of a power failure or mechanical failure of the fan. It would be desirable to have a stack through which waste heat could be dumped and which will create a draft across the heater to aid in the flow of air. It might also be desirable to have a damper system arranged to decrease the flow resistance

of the system should the fan cease operation. Reference (33, p. 1120) gives

$$H_v = 0.52\ P\ H\ \left(\frac{1}{T_{in}} - \frac{1}{T_{out}}\right)$$

for determining the velocity head of a stack where

H_v is the velocity head in inches of water

P is the atmospheric pressure in psia

H is the height of the stack in feet

T_{in} is the absolute air inlet temperature to the heater

T_{out} is the absolute air outlet temperature from the stack.

If the stack height is assumed to be 15 feet, the inlet temperature 70 °F, and the outlet temperature is limited to 300 °F, H_v is 0.0625 inches of water. This value can be used to calculate the velocity, V, that is theoretically possible.

$$V = 1096.5\sqrt{Hv/\rho_{air}} = 1021 \text{ feet per minute or}$$

61,260 feet per hour.

This is nearly twice the previously calculated value necessary to provide the proper coolant flow for operation. This calculation ignores the pressure drop in the free circulation loop. However, if the velocity head is only 0.02 inches of water (allowing 2/3 of the head for pressure drop in the system) the velocity is 34,000 feet per hour and still above that required. It is unlikely that simply shutting off the fan would result in any overheating of the source rods or the shield.

In the case of a fire it is possible that the temperature entering the heater would be much higher for a short time. By carefully locating the heater and ducts the normal circulation should be restored upon cooling down.

In a situation such as a fire it is possible that the duct work to the heater or from the heater could become blocked. If a 700 °F temperature rise above normal operation is assumed to be acceptable, the uranium shield will be near its melting point provided it is perfectly insulated as assumed in the gamma heating calculations. The melting point of the stainless steel or hastelloy will probably not be reached however. It will be further assumed that there is no heat transfer away from the heater. The rate of rise of the temperature can be estimated by making the further assumption that the specific heats of the materials remain relatively constant with temperature.

$$q = W c_p \Delta t$$

where q is the rate at which energy is added to a mass, W, which has a constant pressure specific heat, c_p. The resulting rise is Δt. Rewriting the equation

$$dt = \frac{dq}{W c_p} \quad \text{or} \quad dt = \frac{dq}{\sum (W c_p)} .$$

When the source is new the energy output is about 30 kw. The weights of the various components of the heater can be estimated from the previous design calculations and references (23) and (22) provide the specific heats as given in Table 17.

Table 17. Estimated weights and specific heat of heater components

Component	Weight lb	Specific heat Btu/lb/°F		
		212 °F	440 °F	1162 °F
Shield - U	18,600		0.0577	0.0843
Shield clad stainless steel	315	0.12		
Source - oxides	265	0.2 (estimated for oxides)		
Source cladding hastelloy C	319	0.166		

The sum of the product of the weights and specific heats indicates the temperature rise per hour to be about 63 °F/hr. In other words about 11 hours are available to remove the obstruction and at least restore natural convection if not forced convection. The heat transfered to the surroundings has been ignored as well as the heating of the small amount of other structure within the heater.

In conclusion it appears that the only way the shield will be lost in a short time is by mechanically tearing it off or exposing the cladding and shield to a heat source sufficiently great to cause it to melt.

COST ANALYSIS AND ECONOMICS

By present day prices and standards this will be an expensive source of heat. The question of whether or not it is economical is dependent on many variables, and can be answered only when the locality and conditions of the installation are known. Situations which have high reliability, portability, long life, and low logistics needs may well find the heater economical. An approximation of the original cost at present day prices will be made and some alternatives which could greatly affect costs will be discussed.

The source material exists as a by-product of nuclear reactor operation and should be relatively inexpensive. However, the cost of putting these wastes into vessels as calcined oxides is significant. Reference (10, p. 31) gives costs based on engineering studies for various feed materials (Purex, Thorex, etc.). These costs include the operation of the calcination plant, the capital investments and calcination vessels for preparing waste for storage. A typical number is 0.05 mills per electrical kilowatt hour produced by the reactor fuel which was reprocessed. The source for the fission-product heater requires 4.34 tonnes of uranium with a thermal burnup of 10,000 Mw days/tonne. The cost of getting the source material ready to use in the heater would be about $130,000 assuming the efficiency is 40%. Most of this cost is borne by the power reactor owners. It seems reasonable to expect some of this cost to be charged against the fission product users.

The major item in the cost of the heater is that of the shield. In the interests of maximum portability, small space, and low weight, uranium was chosen as the shield. It will weigh about 9.3 tons. If the cost of casting, machining, and cladding the uranium is assumed to be $5.00 per pound, (the National Lead Co. quotes depleted uranium in the form of sheets, castings, or machined parts costing from $5.00 to $30.00 per pound) the shield cost approaches $95,000.

There are a number of costs of the installation which will be about the same regardless of the material used as a shield. The radioactivity monitoring and warning devices, fans, filter, ductwork, and dampers will be required in any design. The specifications of these pieces of the heating system will likely be more exacting than normal and will incorporate safety features such as fan actuated dampers. It is also likely that these items will form a relatively small portion of the total cost of the heater.

The approximate total cost of the installed heater will be $153,400 broken down as follows

1.	Source, source processing, and source vessels	$50,000
2.	Uranium shielding	95,000
3.	Monitoring and warning devices	3,500
4.	Transportation charges (1500 miles) at $12.00 per 100 pounds	2,400
5.	Miscellaneous equipment (ducts, fans, filters, dampers)	1,500

6.	Foundation and concrete shielding	500
7.	Loading, unloading, and installation	500
	Total	$153,400

Reference (34) gives projected costs for developmental isotopic and nuclear power. The power cost of systems such as SNAP 7a and 7c is about $200.00 per Kw hour. These devices produce about 10 watts. The mobile nuclear reactors such as the ML-1 produce 40 Kw at a cost of about $0.20 per Kw hour. The prediction for devices in the 7.5 Kw range is $2.00 to $3.00 per Kw hour. The reference goes on to say (as others frequently do) that isotopic power sources do not appear competitive. This may be true, especially for electrical generation, however, as a heat source this design could be below the predicted values. If it is assumed that all of the energy above the design output is wasted and the fission-product heater can be installed for the estimated $153,400, the following calculation can be made

$$\text{Power generation} = (7.5 \text{ Kw})(30 \text{ yr})(24 \text{ hr/day})(365 \text{ day/yr})$$
$$= 1.97 \times 10^6 \text{ Kw hr}$$
$$\text{Cost per Kw hr} = \$1.5 \times 10^5 / 1.97 \times 10^6 \text{ Kw hr}$$
$$= \$0.078/\text{Kw hr.}$$

This cost is too high to be competitive in the U.S. for heating purposes but it may be very much in competition in remote areas or space. The calculated value will be decreased if the excess energy is not wasted during the heater's life.

A number of materials could be used for the shield from a biological point of view if space, portability, and weight are not vital. However, the recovery of the energy given up in the shield by photons becomes more difficult as the shield gets larger. For comparison purposes, consider the cost of an equivalent cast iron shield. The iron shield will be considerably larger and weigh more since buildup factors are higher for lighter materials. Reference to some recent calculations by Rohach* shows that the equivalent iron shield would have to be 2.7 times as thick as a uranium shield for a 20,000 curie Co - 60 source. This results in an iron shield weight of 18 tons. If the cost is assumed to be $0.20 per pound, the iron shield would be approximately $7,200. This factor of 13.5 in cost savings may be offset by the increased size and weight of the shield for certain applications. The overall dimensions of the shield would be 48.6 inches outside diameter and 76.5 inches in height. The iron shield has another advantage, however, in that the requirement of cladding is diminished if not eliminated. An iron shield might be a good choice for a shipping cask.

Partial fueling of the heater could result in a savings over the life of the heater. The design output of the heater is 25,000 Btu/hr, however, at the beginning of its operation it produces nearly 100,000 Btu/hr. If one half or one third of the source material was put in place and the remainder added as time went on, there would be a slightly thinner shield required. This saving would not be great and could

*Rohach, A. F., Nuclear Engineering Department, I.S.U., Ames, Iowa. Data from composite U, Fe, and concrete shield calculations. Private communication. 1966.

easily be overshadowed by the increased transportation cost. Reference to the calculations on isotropic point sources (26) shows that a decrease in source strength from 50 Mc to 5 Mc changes the shield thickness from 16.88 cm of uranium for 1.0 mev photons to 15.33 cm. A further decrease to 0.5 Mc only decreases the thickness to 13.79 cm.

Unseparated fission products represent a rapidly enlarging source of energy which can be used. Because of improved waste processing technology the cost of using that energy is not prohibitive. The unique properties of long life with little maintenance make the fission-product heater a good prospect for an economical remote area heat source.

SUMMARY

The fission-product heater is designed to make use of the energy given off by unseparated, radioactive, nuclear reactor fuel wastes which have been calcined. The energy is to be used to heat air to a maximum temperature of 300 °F. The heater is to produce a minimum of 25,000 Btu/hr over a design lifetime of 30 years.

Until the last two or three years, gross fission products have been regarded as unsuitable for power sources because of their low power densities. However, the outlook for making use of these by-products is promising, especially since the technology of calcination is rapidly being developed. With a specific activity of 180,000 curies per pound and a density of 2.4 grams per cm^3 a 47.7 Mc source weighing 265 pounds is sufficiently large to provide the energy requirement for this design. The heat transfer character of the source material is such that a diameter of four inches is about the maximum that can be tolerated and not exceed the melting point at the center of the source. The final configuration for the source material was chosen as seven 4 - inch diameter tubes, three feet in length. Each tube has six external, longitudinal fins and is positioned by inserting it in a coolant channel. The channels are arranged in a close-packed hexagonal array.

If the fission products are permitted to decay for at least two years, the radiation is approximately 90% beta emission. A clad uranium shield of 5.3 inches and weighing 9.3 tons is required to reduce the

surface dose rate to 200 mr/hr. Uranium was selected as the shield material in the interests of low weight, small size and maximum portability. The heat transfer characteristics of the shield are such that gamma heating will not pose a problem.

The potential hazard of this source is great if the shield is destroyed. Loss of coolant flow will not present a serious threat if a stack 15 feet in height is provided and flow actuated dampers decrease the system pressure loss. Enough heat transfer area is provided to permit sufficient cooling by natural convection. In case of a blocked coolant flow an 11 - hour period is required to heat the device to near the melting point of the shield.

It is estimated that the initial cost of producing energy at relatively low temperature levels by means of the fission-product heater is about $0.08 per Kw hr. A device such as this would be suitable for applications such as space heating and distilling water. Considerable reduction in cost could be made by selecting lighter metallic shields and sacrificing space and weight.

There are a number of areas which need to be investigated by experiment before such a device is built. Data are lacking for the source material and for the shielding of large sources. Experimental verification of the shielding calculations for very large sources is also needed. Verification is also needed for the heat transfer correlations.

LITERATURE CITED

1. Rutherford, E. and Barnes, H. T. Heating effect of radium emanation. Philosophical Magazine 7: 202-212. 1904.

2. Isotopic power development. Isotopes and Radiation Technology 1: 325-339. 1964.

3. Fowler, E. E. and Aebersold, P. C. Status of the U.S. program on isotopes and radiation development. Isotopes and Radiation Technology 1: 6-10. 1963.

4. Rohrmann, C. A. Radioisotopic heat sources: supplementary data. U.S. Atomic Energy Commission Report HW-78180 (Hanford Works, Washington). 1963.

5. Rohrmann, C. A. Radioisotopic heat sources: supplementary data. U.S. Atomic Energy Commission Report HW-76323 (Hanford Works, Washington). 1963.

6. Rohrmann, C. A. Isotopic separation as a factor in the selection of candidate heat-source radioisotopes. U.S. Atomic Energy Commission Report HW-78658 (Hanford Works, Washington). 1963.

7. Rohrmann, C. A. The fission products. U.S. Atomic Energy Commission Report HW-SA-3080 (Hanford Works, Washington). 1964.

8. Moore, R. L. Promethium as an isotopic fuel. U.S. Atomic Energy Commission Report HW-82215 (Hanford Works, Washington). 1964.

9. Rohrmann, C. A. The fission products. U.S. Atomic Energy Commission Report TID-7698 (Division of Technical Information). Part 1: 1-16. 1964.

10. Perona, J. J., Bradshaw, R. L., Roberts, J. T. and Blomeke, J. O. Evaluation of ultimate disposal methods for liquid and solid radioactive wastes. Part 2. Conversion to solid by pot calcination. U.S. Atomic Energy Commission Report ORNL-3192 (Oak Ridge National Laboratory, Tennessee). 1961.

11. Corliss, W. R. and Harvey, D. G. Radioisotopic power generation. Englewood Cliffs, N. J., Prentice Hall, Inc. 1964.

12. Barnes, W. H., Light, L. E. and Totah, A. A. Feasibility study of a radioisotope power source for remote area heating. U.S. Atomic Energy Commission Report AD-276451 (Defense Documentation Center, Va.). 1962.

13. Availability of isotopes and services. Isotopes and Radiation Technology 3: 79. 1965.

14. Chance Vought Corporation. Utilization of isotopes for saline water conversion. U.S. Department of the Interior Report PB-181469 (Office of Technical Services). 1962.

15. Eaton, D. Development of techniques for power production from mixed fission products. U.S. Atomic Energy Commission Report NYO-9699 (New York Operations office). 1962.

16. Posey, J. C. and Motlenry, R. E. Heat transfer in the design of large radioisotopic heat sources. U.S. Atomic Energy Commission Report ORNL-P-1945 (Oak Ridge National Laboratory, Tennessee). 1966.

17. VanTuyl, H. H. Fission product radiation and shielding calculations. U.S. Atomic Energy Commission Report HW-69533 (Hanford Works, Washington). 1961.

18. Arnold, E. D. Shielding requirements for isotopic power sources. U.S. Atomic Energy Commission Report ORNL-3576 (Oak Ridge National Laboratory, Tennessee). 1964.

19. Blomeke, J. O. and Todd, M. F. Uranium-235 fission product production as a function of thermal neutron flux, irradiation time, and decay time. U.S. Atomic Energy Commission Report ORNL-2127 (Oak Ridge National Laboratory, Tennessee). 1957.

20. Perona, J. J. The effects of internal heat generation on pot calcination rates for radioactive wastes. U.S. Atomic Energy Commission Report ORNL-3163 (Oak Ridge National Laboratory, Tennessee). 1961.

21. Trent Tube Company. Hastelloy alloy C data sheet. Trent Tube Company (East Troy, Wisconsin) Issue No. 2 ca. 1960.

22. American Society of Mechanical Engineers. ASME handbook of metal properties. 1st edition. New York, New York, McGraw Hill Book Company, Incorporated. 1954.

23. American Society for Metals. Metals handbook. Vol. 1. Novelty, Ohio, author. 1961.

24. Blizard, E. P., editor. Reactor handbook. 2nd edition. Vol. 3. Part B. Shielding. New York, New York, Interscience Publishers. 1962.

25. Argonne National Laboratory. Reactor physics constants. 2nd edition. U.S. Atomic Energy Commission Report ANL-5800 (Argonne National Laboratory, Illinois). 1963.

26. Moser, J. S. Shielding properties of the UPb_3 intermetallic compound. Unpublished M. S. thesis. Ames, Iowa, Library, Iowa State University of Science and Technology. 1966.

27. Glasstone, S. and Sesonske, A. Nuclear reactor engineering. Princeton, New Jersey, D. Van Nostrand Company, Inc. 1963.

28. Kreith, F. Principles of heat transfer. 2nd edition. Scranton, Penna., International Textbook Company. 1965.

29. Fortescue, P. and Hall, W. B. Heat-transfer experiments on the fuel elements. Symposium: Calder works nuclear power plant. British Nuclear Energy Conference Journal 2, No. 2: 83-91. 1957.

30. Obert, E. and Young, R. L. Elements of thermodynamics and heat transfer. 2nd edition. New York, New York, McGraw-Hill Book Company, Inc. 1962.

31. McAdams, W. H. Heat transmission. 3rd edition. New York, New York, McGraw-Hill Book Company, Inc. 1954.

32. Jakob, M. Heat transfer. Vol. 1. New York, New York, John Wiley and Sons, Inc. 1958.

33. Marks, Lionel S., editor Mechanical engineers handbook. 5th edition. New York, New York, McGraw-Hill Book Co., Inc. 1951.

34. Cohn, Paul D. From watts to megawatts with packaged nuclear power. Power Engineering 70, No. 2: 50-53. 1966.

ACKNOWLEDGMENTS

The author wishes to acknowledge the faith and encouragement of his wife Shirley, and his family. Without their cooperation this work would not have been possible.

Sincere thanks and appreciation is extended to Dr. Glenn Murphy for initially suggesting this project and for his timely help and guidance during the detailed work.

Thanks is gratefully extended to the Ford Foundation and the Forgivable Loan Program, administered by I.S.U. for financial support.

Finally, thanks is due to those who worked in the author's absence to permit his extended leave from the University of North Dakota.

APPENDIX

Calculations and Tabulated Results for Biological Shielding

The calculations summarized herein were done for each of the seven source tubes shown in Figure 10 and for three shield thicknesses (points D, E, and F). The photon spectrum was assumed to exist as four distinct energy groups. Figure 19 gives the arrangement for which the calculation was made. Values of the distance from the point under consideration to the source and the shield thickness were measured from the scale drawing of Figure 10. Reference (24) was used to evaluate the secant integrals and to determine the source self-absorption distances. The energy flux was calculated from the following relation:

$$\phi_e = \frac{S_v r^2}{4 (z + t_c)} \; 2 \left[F (\theta, \mu t + \mu_c t_c) \right] .$$

where

S_v is the source strength in mev/cm^3/sec

r is the source radius in cm

z is the distance from the point under consideration to the source in cm

t_c is the source self absorption distance in cm

t is the shield thickness in cm

μ_c is the attenuation coefficient for the source in 1/cm

μ is the attenuation coefficient for the shield in 1/cm

$F(\theta, \mu t + \mu t_c)$ is the secant integral

The results of these calculations are tabulated in Table 18.

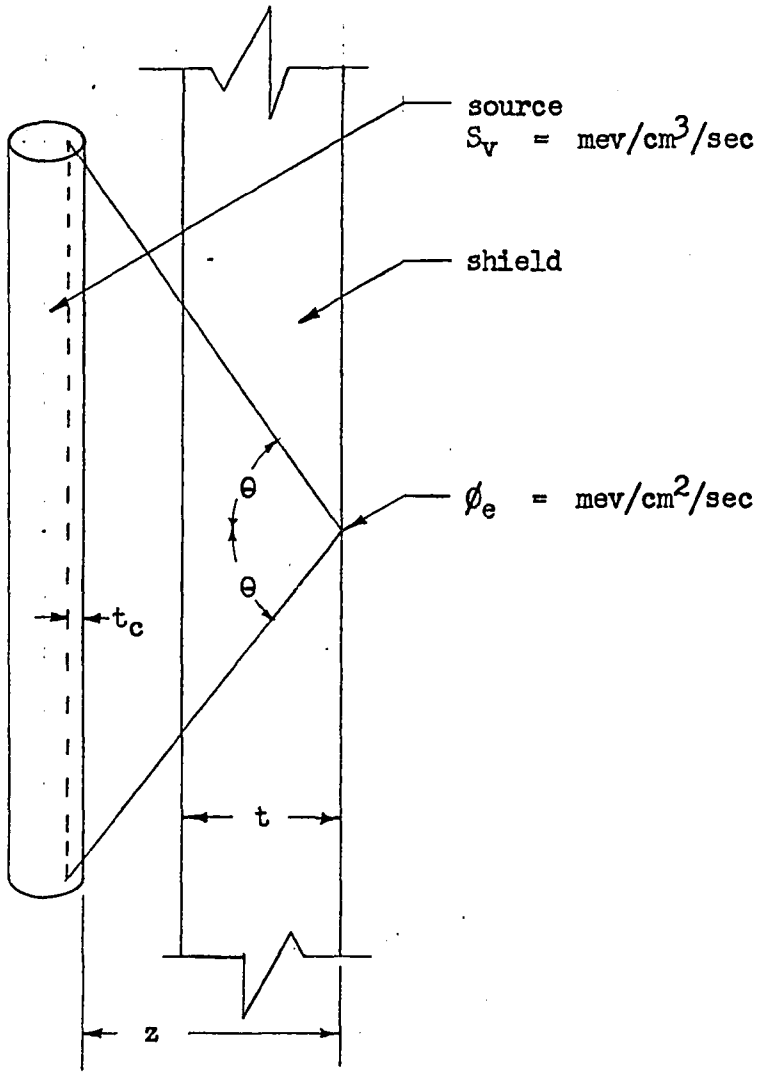

Figure 19. Source and shield arrangement for shielding calculations.

Table 18. Tabulated results for Figure 10

Source	Photon group & energy	z cm	t cm	t_c cm	θ degrees	S_v $\frac{mev}{cm^3 sec}$	z + t_c cm	F(θ, μt)	ϕ_e $\frac{mev}{cm^2 sec}$
Point E - 2.5-inch shield									
0	I-0.125	26.9	6.35	3.3	30.5	$9.88X10^9$	30.2	$<10^{-10}$	0.42
	II-0.67	26.9	6.35	3.58	30.5	$7.72X10^{10}$	30.5	$1.2X10^{-8}$	$3.92X10^2$
	III-1.6	26.9	6.35	4.41	30.5	$7.54X10^9$	31.3	$2.1X10^{-4}$	$6.52X10^5$
	IV-2.4	26.9	6.35	4.29	30.5	$4.21X10^9$	31.2	$2.27X10^{-3}$	$2.27X10^6$
1	I-0.125	9.77	6.35	3.71	12.1	$9.88X10^9$	13.4	$<10^{-10}$	0.952
	II-0.67	9.77	6.35	4.42	12.1	$7.72X10^{10}$	14.1	$6.55X10^{-9}$	$4.59X10^3$
	III-1.6	9.77	6.35	4.62	12.1	$7.54X10^9$	14.3	$1.8X10^{-4}$	$1.224X10^6$
	IV-2.4	9.77	6.35	4.65	12.1	$4.21X10^9$	14.3	$6.5X10^{-4}$	$2.47X10^6$
2 & 6	I-0.125	22.75	8.0	3.6	26.5	$9.88X10^9$	26.3	$<10^{-10}$	0.485
	II-0.67	22.75	8.0	3.94	26.5	$7.72X10^{10}$	26.6	$1.6X10^{-10}$	5.98
	III-1.6	22.75	8.0	4.26	26.5	$7.54X10^9$	27.0	10^{-6}	$3.6X10^3$
	IV-2.4	22.75	8.0	4.45	26.5	$4.21X10^9$	27.15	$4X10^{-6}$	$8.01X10^3$
3 & 5	I-0.125	38	6.98	2.59	39.7	$9.88X10^9$	40.59	$<10^{-10}$	0.314
	II-0.67	38	6.98	3.71	39.7	$7.72X10^{10}$	41.7	$2.3X10^{-9}$	5.49X10
	III-1.6	38	6.98	3.35	39.7	$7.54X10^9$	41.35	$1.95X10^{-4}$	$4.69X10^5$
	IV-2.4	38	6.98	3.57	39.7	$4.21X10^9$	41.57	$9.4X10^{-4}$	$12.25X10^5$
4	I-0.125	44	6.35	2.27	43.9	$9.88X10^9$	46.27	$<10^{-10}$	0.276
	II-0.67	44	6.35	3.55	43.9	$7.72X10^{10}$	47.55	$1.25X10^{-8}$	$2.62X10^2$
	III-1.6	44	6.35	3.17	43.9	$7.54X10^9$	47.17	$4.5X10^{-4}$	$9.28X10^5$
	IV-2.4	44	6.35	3.1	43.9	$4.21X10^9$	47.1	$1.7X10^{-3}$	$1.96X10^6$

ϕ_{total} $1.12X10^7$ mev/cm²/sec

Table 18 (Continued)

Source	Photon group & energy	z cm	t cm	t_c cm	θ degrees	S_v $\frac{mev}{cm^3 sec}$	z + t_c cm	F(θ, μt)	ϕ_e $\frac{mev}{cm^2 sec}$
Point E - 5-inch shield									
0	I-0.125	33.1	12.7	2.89	36	$9.88X10^9$	35.99	$<10^{-10}$	$3.55X10^{-1}$
	II-0.67	33.1	12.7	3.43	36	$7.72X10^{10}$	36.53	$<10^{-10}$	2.73
	III-1.6	33.1	12.7	3.78	36	$7.54X10^9$	36.88	$4.4X10^{-7}$	$1.16X10^3$
	IV-2.4	33.1	12.7	4.31	36	$4.21X10^9$	37.41	$5.3X10^{-6}$	$7.67X10^3$
1	I-0.125	16.12	12.7	3.55	19.5	$9.88X10^9$	19.67	$<10^{-10}$	$6.48X10^{-1}$
	II-0.67	16.12	12.7	4.11	19.5	$7.72X10^{10}$	20.23	$<10^{-10}$	4.91
	III-1.6	16.12	12.7	4.63	19.5	$7.54X10^9$	20.75	$2.8X10^{-7}$	$1.31X10^3$
	IV-2.4	16.12	12.7	4.71	19.5	$4.21X10^9$	20.83	$4.1X10^{-6}$	$1.07X10^4$
2 & 7	I-0.125	28.2	15.5	3.52	31.6	$9.88X10^9$	31.72	$<10^{-10}$	$4.02X10^{-1}$
	II-0.67	28.2	15.5	3.86	31.6	$7.72X10^{10}$	32.06	$<10^{-10}$	3.11
	III-1.6	28.2	15.5	4.38	31.6	$7.54X10^9$	32.58	$2.1X10^{-8}$	6.26X10
	IV-2.4	28.2	15.5	4.68	31.6	$4.21X10^9$	32.88	$4.6X10^{-7}$	$7.6X10^2$
3 & 6	I-0.125	43.9	13.6	2.27	43.8	$9.88X10^9$	46.17	$<10^{-10}$	$2.765X10^{-1}$
	II-0.67	43.9	13.6	3.23	43.8	$7.72X10^{10}$	47.13	$<10^{-10}$	2.11
	III-1.6	43.9	13.6	3.04	43.8	$7.54X10^9$	46.94	$2X10^{-7}$	$4.15X10^2$
	IV-2.4	43.9	13.6	3.23	43.8	$4.21X10^9$	47.13	$2.8X10^{-6}$	$3.22X10^3$
4	I-0.125	50.2	12.7	2.84	47.7	$9.88X10^9$	53.04	$<10^{-10}$	$2.405X10^{-1}$
	II-0.67	50.2	12.7	2.41	47.7	$7.72X10^{10}$	52.61	$<10^{-10}$	1.89
	III-1.6	50.2	12.7	2.32	47.7	$7.54X10^9$	52.52	$5.5X10^{-7}$	$1.018X10^3$
	IV-2.4	50.2	12.7	2.38	47.7	$4.21X10^9$	52.58	$7X10^{-6}$	$7.22X10^3$

ϕ_{total} $3.46X10^4$ mev/cm²/sec

Table 18 (Continued)

Source	Photon group & energy	z cm	t cm	t_c cm	θ degrees	S_v $\frac{\text{mev}}{\text{cm}^3\text{sec}}$	z + t_c cm	F(θ, μt)	ϕ_e $\frac{\text{mev}}{\text{cm}^2\text{sec}}$
Point F - 7.5-inch shield									
0	I-0.125	39.6	19.05	2.67	41	9.88×10^{9}	41.27	$<10^{-10}$	3.09×10^{-1}
	II-0.67	39.6	19.05	3.61	41	7.72×10^{10}	43.21	$<10^{-10}$	2.31
	III-1.6	39.6	19.05	3.24	41	7.54×10^{9}	42.84	6.5×10^{-10}	1.475
	IV-2.4	39.6	19.05	3.26	41	4.21×10^{9}	42.86	2.8×10^{-8}	35.5
1	I-0.125	22.45	19.05	3.71	26.3	9.88×10^{9}	26.16	$<10^{-10}$	4.88×10^{-1}
	II-0.67	22.45	19.05	3.98	26.3	7.72×10^{10}	26.43	$<10^{-10}$	3.765
	III-1.6	22.45	19.05	4.45	26.3	7.54×10^{9}	26.9	5.5×10^{-10}	1.99
	IV-2.4	22.45	19.05	4.61	26.3	4.21×10^{9}	27.06	2.5×10^{-8}	50.2
2 & 6	I-0.125	34	22.2	2.9	36.6	9.88×10^{9}	36.9	$<10^{-10}$	3.45×10^{-1}
	II-0.67	34	22.2	3.64	36.6	7.72×10^{10}	37.64	$<10^{-10}$	2.65
	III-1.6	34	22.2	3.44	36.6	7.54×10^{9}	37.44	$<10^{-10}$	2.6×10^{-1}
	IV-2.4	34	22.2	3.83	36.6	4.21×10^{9}	37.83	1.8×10^{-9}	2.59
3 & 5	I-0.125	50.15	20.45	2.72	47.6	9.88×10^{9}	52.87	$<10^{-10}$	2.41×10^{-1}
	II-0.67	50.15	20.45	2.89	47.6	7.72×10^{10}	53.04	$<10^{-10}$	1.88
	III-1.6	50.15	20.45	2.32	47.6	7.54×10^{9}	52.47	1.7×10^{-10}	3.15
	IV-2.4	50.15	20.45	2.47	47.6	4.21×10^{9}	52.62	9.5×10^{-9}	9.8
4	I-0.125	57	19.05	2.72	51.2	9.88×10^{9}	59.72	$<10^{-10}$	2.14×10^{-1}
	II-0.67	57	19.05	2.89	51.2	7.72×10^{10}	59.89	$<10^{-10}$	1.67
	III-1.6	57	19.05	2.32	51.2	7.54×10^{9}	59.32	7.5×10^{-10}	1.23
	IV-2.4	57	19.05	2.47	51.2	4.21×10^{9}	59.47	3.4×10^{-8}	31.1
								ϕ_{total}	1.51×10^{2} mev/cm²/sec

Calculations and Tabulated Results for End Slab Shields

For these calculations the source materials was assumed to be a volume distributed source which occupies the entire central region of the heater. The calculation was done for two thicknesses and for four photon energy groups as before. Tabulations given in reference (24) were used to evaluate the various exponential integrals which appear in the equation. The relation used to calculate the energy flux is

$$\phi_e = \frac{S_v}{2\mu_c}\left(\left[E_2(\mu t) - \cos\theta\, E_2(\mu t \sec\theta)\right] - \left[E_2(\mu t + \mu_c h) - \cos\theta\, E_2\left\{(\mu t + \mu_c h)\sec\theta\right\}\right]\right).$$

where h is the length of the cylindrical source and E_2 ( ) is the exponential integral. All other symbols are as given in the previous appendix or as shown in Figure 20. The results of these calculations are given in Table 19 and are plotted in Figure 11.

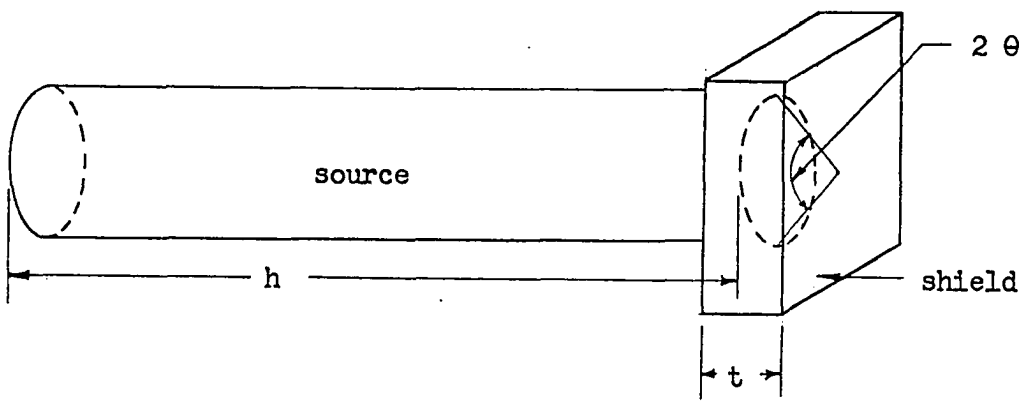

Figure 20. Source and shield arrangement for end slab shield calculations.

Table 19. Tabulated results for end slab shields

Photon group and energy mev	h cm	μ_c 1/cm	μ 1/cm	t cm	θ degrees	S_v $\frac{\text{mev}}{\text{cm}^3\ \text{sec}}$	ϕ_e $\frac{\text{mev}}{\text{cm}^2\ \text{sec}}$
I-0.125	91.5	0.405	62.4	12.7	63.4	9.88×10^9	< 0.122
II-0.67	91.5	0.208	2.55	12.7	63.4	7.72×10^{10}	< 1.855
III-1.6	91.5	0.1295	1.02	12.7	63.4	7.54×10^9	4.66×10^3
IV-2.4	91.5	0.1052	0.831	12.7	63.4	4.21×10^9	4.21×10^4
					ϕ_e Total =	4.68×10^4 mev/cm^2/sec	
I-0.125	91.5	0.405	62.4	6.35	75.8	9.88×10^9	< 0.122
II-0.67	91.5	0.208	2.55	6.35	75.8	7.72×10^{10}	< 1.855
III-1.6	91.5	0.1295	1.02	6.35	75.8	7.54×10^9	5.53×10^6
IV-2.4	91.5	0.1052	0.831	6.35	75.8	4.21×10^9	1.42×10^6
					ϕ_e Total =	6.95×10^6 mev/cm^2/sec	

Calculations and Tabulated Results for Gamma Heating

The calculations summarized in this appendix were done for each of the seven source tubes as shown in Figure 10 and for six different depths into the shield from the inside surface. The equation of the biological shielding appendix and Figure 19 apply to this calculation.

The results for 0.0, 0.1, 0.2, 0.5, and 1.0 cm depth into the shield are tabulated in Table 20. The results for 6.35 cm depth is included in Table 18. Table 21 gives the tabulated results for Figure 17.

Table 20. Tabulated results for gamma heating calculations.

Source	Photon group & energy	z cm	t cm	t_c cm	θ degrees	S_v $\frac{mev}{cm^3 sec}$	z + t_c cm	F(θ, μt)	ϕ_e $\frac{mev}{cm^2 sec}$
Depth into shield is 0.0 cm									
0	I-0.125	20.58	0	3.5	>50	$9.88X10^9$	21.99	0.19	$1.1X10^9$
	II-0.67	20.58	0	3.66	50	$7.72X10^{10}$	21.34	0.42	$1.96X10^{10}$
	III-1.6	20.58	0	4.17	50	$7.54X10^9$	21.12	0.56	$2.58X10^9$
	IV-2.4	20.58	0	4.42	50	$4.21X10^9$	21.05	0.65	$1.68X10^9$
1	I-0.125	3.43	0	0.42	>50	$9.88X10^9$	3.60	1.1	$3.9X10^{10}$
	II-0.67	3.43	0	0.654	50	$7.72X10^{10}$	3.57	1.15	$3.2X10^{11}$
	III-1.6	3.43	0	0.788	50	$7.54X10^9$	3.53	1.2	$3.3X10^{10}$
	IV-2.4	3.43	0	0.323	50	$4.21X10^9$	3.46	1.3	$2.04X10^{10}$
2 & 6	I-0.125	16.85	0	3.43	>50	$9.88X10^9$	18.24	0.185	$1.295X10^9$
	II-0.67	16.85	0	3.86	50	$7.72X10^{10}$	17.65	0.41	$2.32X10^{10}$
	III-1.6	16.85	0	4.13	50	$7.54X10^9$	17.39	0.6	$3.36X10^9$
	IV-2.4	16.85	0	4.12	50	$4.21X10^9$	17.28	0.71	$2.235X10^9$
3 & 5	I-0.125	32.0	0	3.14	>50	$9.88X10^9$	33.27	0.22	$8.43X10^8$
	II-0.67	32.0	0	3.54	50	$7.72X10^{10}$	32.74	0.42	$1.28X10^{10}$
	III-1.6	32.0	0	3.62	50	$7.54X10^9$	32.47	0.58	$1.732X10^9$
	IV-2.4	32.0	0	3.88	50	$4.21X10^9$	32.41	0.61	$1.022X10^9$
4	I-0.125	37.5	0	2.72	>50	$9.88X10^9$	38.6	0.25	$8.26X10^8$
	II-0.67	37.5	0	3.57	50	$7.72X10^{10}$	38.24	0.35	$9.1X10^9$
	III-1.6	37.5	0	3.06	50	$7.54X10^9$	37.9	0.54	$1.385X10^9$
	IV-2.4	37.5	0	3.42	50	$4.21X10^9$	37.86	0.6	$8.61X10^9$
								ϕ_{total}	$5.49X10^{11}$ mev/cm²/sec

Table 20 (Continued)

Source	Photon group & energy	z cm	t cm	t_c cm	θ degrees	S_v $\frac{\text{mev}}{\text{cm}^3\text{sec}}$	z + t_c cm	$F(\theta,\mu t)$	ϕ_e $\frac{\text{mev}}{\text{cm}^2\text{sec}}$
Depth into shield is 0.1 cm									
0	I-0.125	20.68	0.1	3.68	>50	9.88×10^{9}	24.36	1.8×10^{-4}	9.4×10^{5}
	II-0.67	20.68	0.1	3.62	50	7.72×10^{10}	24.30	0.32	1.31×10^{10}
	III-1.6	20.68	0.1	4.12	50	7.54×10^{9}	24.80	0.5	1.96×10^{9}
	IV-2.4	20.68	0.1	4.37	50	4.21×10^{9}	25.05	0.6	1.3×10^{9}
1	I-0.125	3.53	0.1	0.518	>50	9.88×10^{9}	4.05	6.8×10^{-4}	2.14×10^{7}
	II-0.67	3.53	0.1	0.757	50	7.72×10^{10}	4.29	0.72	1.67×10^{11}
	III-1.6	3.53	0.1	0.667	50	7.54×10^{9}	4.20	1.0	2.32×10^{10}
	IV-2.4	3.53	0.1	0.327	50	4.21×10^{9}	3.86	1.4	1.97×10^{10}
2 & 6	I-0.125	16.9	0.1	3.9	>50	9.88×10^{9}	20.8	1.6×10^{-4}	9.8×10^{5}
	II-0.67	16.9	0.1	3.75	50	7.72×10^{10}	20.65	0.3	1.445×10^{10}
	III-1.6	16.9	0.1	4.05	50	7.54×10^{9}	20.95	0.52	2.41×10^{9}
	IV-2.4	16.9	0.1	4.07	50	4.21×10^{9}	20.97	0.62	1.605×10^{9}
3 & 5	I-0.125	32.1	0.1	3.28	>50	9.88×10^{9}	35.38	2×10^{-4}	7.2×10^{5}
	II-0.67	32.1	0.1	3.44	50	7.72×10^{10}	35.54	0.3	8.4×10^{9}
	III-1.6	32.1	0.1	3.51	50	7.54×10^{9}	35.61	0.46	1.255×10^{9}
	IV-2.4	32.1	0.1	3.76	50	4.21×10^{9}	35.86	0.52	7.86×10^{8}
4	I-0.125	37.6	0.1	2.98	>50	9.88×10^{9}	40.58	2.3×10^{-4}	7.21×10^{5}
	II-0.67	37.6	0.1	3.7	50	7.72×10^{10}	41.3	0.28	6.75×10^{9}
	III-1.6	37.6	0.1	3.18	50	7.54×10^{9}	40.78	0.48	1.145×10^{9}
	IV-2.4	37.6	0.1	3.55	50	4.21×10^{9}	41.15	0.52	6.86×10^{8}
								ϕ_{total}	3.72×10^{11} mev/cm²/sec

Table 20 (Continued)

Source	Photon group & energy	z cm	t cm	t_c cm	θ degrees	S_v $\frac{mev}{cm^3 sec}$	z + t_c cm	F(θ, μt)	ϕ_e $\frac{mev}{cm^2 sec}$
Depth into shield is 0.2 cm									
0	I-0.125	20.78	0.2	3.9	~62	9.88×10^9	24.68	2.5×10^{-7}	1.292×10^3
	II-0.67	20.78	0.2	3.58	62	7.72×10^{10}	24.36	0.23	9.42×10^9
	III-1.6	20.78	0.2	4.12	62	7.54×10^9	24.90	0.46	1.8×10^9
	IV-2.4	20.78	0.2	4.37	62	4.21×10^9	25.15	0.51	1.1×10^9
1	I-0.125	3.63	0.2	0.52	>84	9.88×10^9	4.15	10^{-6}	3.08×10^4
	II-0.67	3.63	0.2	0.664	84	7.72×10^{10}	4.29	0.52	1.21×10^{11}
	III-1.6	3.63	0.2	0.525	84	7.54×10^9	4.15	0.9	2.11×10^{10}
	IV-2.4	3.63	0.2	0.323	84	4.21×10^9	3.95	1.0	1.375×10^{10}
2 & 6	I-0.125	16.95	0.2	3.865	~65.5	9.88×10^9	20.82	2.6×10^{-7}	1.59×10^3
	II-0.67	16.95	0.2	4.12	65.5	7.72×10^{10}	21.07	0.19	8.97×10^9
	III-1.6	16.95	0.2	4.42	65.5	7.54×10^9	21.37	0.44	2.0×10^9
	IV-2.4	16.95	0.2	4.38	65.5	4.21×10^9	21.33	0.51	1.3×10^9
3 & 5	I-0.125	32.2	0.2	3.28	~52	9.88×10^9	35.48	3.2×10^{-7}	1.15×10^3
	II-0.67	32.2	0.2	3.38	52	7.72×10^{10}	35.58	0.25	7.01×10^9
	III-1.6	32.2	0.2	5.46	52	7.54×10^9	37.66	0.51	1.315×10^9
	IV-2.4	32.2	0.2	3.77	52	4.21×10^9	35.47	0.58	8.75×10^8
4	I-0.125	37.7	0.2	2.83	~48	9.88×10^9	40.5	3.9×10^{-7}	1.23×10^3
	II-0.67	37.7	0.2	3.50	48	7.72×10^{10}	41.2	0.21	5.075×10^9
	III-1.6	37.7	0.2	3.01	48	7.54×10^9	40.7	0.45	1.075×10^9
	IV-2.4	37.7	0.2	3.35	48	4.21×10^9	41.05	0.5	6.6×10^8
							ϕ_{total}	2.161×10^{11} mev/cm²/sec	

Table 20 (Continued)

Source	Photon group & energy	z cm	t cm	t_c cm	θ degrees	S_v $\frac{mev}{cm^3 sec}$	z + t_c cm	$F(\theta, \mu t)$	ϕ_e $\frac{mev}{cm^2 sec}$
Depth into shield is 0.5 cm									
0	I-0.125	21.08	0.5	3.38	62	9.88×10^9	24.46	10^{-10}	5.21×10^{-1}
	II-0.67	21.08	0.5	3.63	62	7.72×10^{10}	24.71	9.2×10^{-2}	3.71×10^9
	III-1.6	21.08	0.5	4.16	62	7.54×10^9	25.24	2.9×10^{-1}	1.115×10^9
	IV-2.4	21.08	0.5	4.27	62	4.21×10^9	25.35	3.7×10^{-1}	7.93×10^8
1	I-0.125	3.93	0.5	0.488	> 84	9.88×10^9	4.42	10^{-10}	2.88×10^6
	II-0.67	3.93	0.5	0.605	84	7.72×10^{10}	4.54	0.18	3.95×10^{10}
	III-1.6	3.93	0.5	0.405	84	7.54×10^9	4.34	0.56	1.255×10^{10}
	IV-2.4	3.93	0.5	0.332	84	4.21×10^9	4.26	0.6	7.65×10^9
2 & 6	I-0.125	17.10	0.5	3.75	65.5	9.88×10^9	20.85	10^{-10}	6.11×10^{-1}
	II-0.67	17.10	0.5	3.75	65.5	7.72×10^{10}	20.85	0.09	4.3×10^9
	III-1.6	17.10	0.5	4.42	65.5	7.54×10^9	21.52	0.29	1.31×10^9
	IV-2.4	17.10	0.5	4.38	65.5	4.21×10^9	21.48	0.35	8.85×10^8
3 & 5	I-0.125	32.5	0.5	3.28	52	9.88×10^9	35.8	10^{-10}	3.56×10^{-1}
	II-0.67	32.5	0.5	3.56	52	7.72×10^{10}	36.1	0.095	2.62×10^9
	III-1.6	32.5	0.5	3.34	52	7.54×10^9	35.84	0.33	8.95×10^8
	IV-2.4	32.5	0.5	3.65	52	4.21×10^9	36.15	0.38	5.71×10^8
4	I-0.125	38	0.5	2.59	48.4	9.88×10^9	40.59	10^{-10}	3.14×10^{-1}
	II-0.67	38	0.5	3.68	48.4	7.72×10^{10}	41.68	0.085	2.03×10^9
	III-1.6	38	0.5	3.14	48.4	7.54×10^9	41.14	0.32	7.56×10^8
	IV-2.4	38	0.5	3.39	48.4	4.21×10^9	41.39	0.35	4.6×10^8
							ϕ_{total}	8.99×10^{10} mev/cm²/sec	

Table 20 (Continued)

Source	Photon group & energy	z cm	t cm	t_c cm	θ degrees	S_v $\frac{mev}{cm^3 sec}$	z + t_c cm	F(θ, μt)	ϕ_e $\frac{mev}{cm^2 sec}$
Depth into shield is 1.0 cm									
0	I-0.125	21.58	1.0	3.42	~61.3	9.88×10^9	25	10^{-10}	5.1×10^{-1}
	II-0.67	21.58	1.0	3.73	61.3	7.72×10^{10}	25.31	2.2×10^{-2}	8.66×10^8
	III-1.6	21.58	1.0	4.17	61.3	7.54×10^9	25.75	1.7×10^{-1}	6.42×10^8
	IV-2.4	21.58	1.0	4.19	61.3	4.21×10^9	25.77	2.2×10^{-1}	4.64×10^8
1	I-0.125	4.43	1.0	0.489	~83.8	9.88×10^9	4.92	10^{-10}	2.59
	II-0.67	4.43	1.0	0.606	83.8	7.72×10^{10}	5.04	4.4×10^{-2}	8.7×10^9
	III-1.6	4.43	1.0	0.382	83.8	7.54×10^9	4.81	2.8×10^{-1}	5.65×10^9
	IV-2.4	4.43	1.0	0.314	83.8	4.21×10^9	4.74	3.6×10^{-1}	4.13×10^9
2 & 6	I-0.125	17.65	1.0	3.43	~65.3	9.88×10^9	21.08	10^{-10}	6.05×10^{-1}
	II-0.67	17.65	1.0	3.8	65.3	7.72×10^{10}	21.45	2×10^{-2}	9.28×10^8
	III-1.6	17.65	1.0	4.25	65.3	7.54×10^9	21.90	1.6×10^{-1}	7.11×10^8
	IV-2.4	17.65	1.0	3.99	65.3	4.21×10^9	21.64	2.2×10^{-1}	5.52×10^8
3 & 5	I-0.125	33.0	1.0	3.08	~51.8	9.88×10^9	36.08	10^{-10}	3.53×10^{-1}
	II-0.67	33.0	1.0	3.29	51.8	7.72×10^{10}	36.3	2.3×10^{-2}	6.36×10^8
	III-1.6	33.0	1.0	3.35	51.8	7.54×10^9	36.35	1.8×10^{-1}	4.82×10^8
	IV-2.4	33.0	1.0	3.59	51.8	4.21×10^9	36.59	2.2×10^{-1}	3.27×10^8
4	I-0.125	38.5	1.0	2.595	~48	9.88×10^9	41.1	10^{-10}	3.1×10^{-1}
	II-0.67	38.5	1.0	3.685	48	7.72×10^{10}	42.2	2.1×10^{-2}	4.96×10^8
	III-1.6	38.5	1.0	3.1	48	7.54×10^9	41.6	1.8×10^{-1}	4.2×10^8
	IV-2.4	38.5	1.0	3.345	48	4.21×10^9	41.85	2.2×10^{-1}	2.86×10^8
								ϕ_{total}	2.895×10^{10} mev/cm2/sec

Table 21. Tabulated results for Figure 17

Photon group and energy mev	Energy flux ϕ_e mev/cm^3/sec	μ_e 1/cm	Energy buildup factor	Depth into shield cm	Energy deposited mev/cm^3/sec
I-0.125	4.51×10^{10}	78.7	1.00	0.0	3.55×10^{12}
II-0.67	4.21×10^{11}	1.52	1.00	0.0	6.40×10^{11}
III-1.6	4.72×10^{10}	0.63	1.00	0.0	2.97×10^{10}
IV-2.4	3.71×10^{10}	0.61	1.00	0.0	2.25×10^{10}
			Total energy deposited	=	4.24×10^{12} mev/cm^3/sec
I-0.125	2.64×10^{7}	78.7	1.25	0.1	2.60×10^{9}
II-0.67	2.31×10^{11}	1.52	1.25	0.1	4.39×10^{11}
III-1.6	3.37×10^{10}	0.63	1.25	0.1	2.66×10^{10}
IV-2.4	2.65×10^{10}	0.61	1.25	0.1	2.01×10^{10}
			Total energy deposited	=	4.89×10^{11} mev/cm^3/sec
I-0.125	3.89×10^{4}	78.7	1.50	0.2	4.60×10^{6}
II-0.67	1.67×10^{11}	1.52	1.25	0.2	3.17×10^{11}
III-1.6	3.06×10^{10}	0.63	1.25	0.2	2.41×10^{10}
IV-2.4	2.00×10^{10}	0.61	1.25	0.2	1.51×10^{10}
			Total energy deposited	=	3.56×10^{11} mev/cm^3/sec
I-0.125	5.65	78.7	1.50	0.5	6.67×10^{2}
II-0.67	5.9×10^{10}	1.52	1.50	0.5	1.34×10^{11}
III-1.6	1.88×10^{10}	0.63	1.50	0.5	1.48×10^{10}
IV-2.4	1.18×10^{10}	0.61	1.50	0.5	8.92×10^{9}
			Total energy deposited	=	1.58×10^{11} mev/cm^3/sec

Table 21 (Continued)

Photon group and energy mev	Energy flux ϕ_e mev/cm^3/sec	μ_e 1/cm	Energy buildup factor	Depth into shield cm	Energy deposited mev/cm^3/sec
I-0.125	5.33	78.7	----	1.0	4.20×10^{2}
II-0.67	1.32×10^{10}	1.52	1.75	1.0	3.51×10^{10}
III-1.6	9.09×10^{9}	0.63	1.32	1.0	7.56×10^{9}
IV-2.4	6.64×10^{9}	0.61	1.32	1.0	5.30×10^{9}
			Total energy deposited =		4.80×10^{10} mev/cm^3/sec
I-0.125	3.25	78.7	----	6.35	2.56×10^{2}
II-0.67	5.3×10^{3}	1.52	----	6.35	8.05×10^{3}
III-1.6	3.74×10^{6}	0.63	3.5	6.35	8.25×10^{6}
IV-2.4	9.16×10^{6}	0.61	3.25	6.35	1.80×10^{7}
			Total energy deposited =		2.63×10^{7} mev/cm^3/sec